Article

Not peer-reviewed version

Capability of New Modified EWMA Control Chart for Integrated and Fractionally Integrated Time Series: Application to US Stock Prices

Kotchaporn Karoon and Yupaporn Areepong *

Posted Date: 2 December 2025

doi: 10.20944/preprints202512.0072.v1

Keywords: average run length; autoregressive Fractionally Integrated; control chart; numerical integral equation; statistical process control

Article

Capability of New Modified EWMA Control Chart for Integrated and Fractionally Integrated Time Series: Application to US Stock Prices

Kotchaporn Karoon [1] and Yupaporn Areepong [2,*]

[1] Department of Mathematics, Faculty of Science, Naresuan University, Phitsanulok, 65000, Thailand
[2] Department of Applied Statistics, Faculty of Applied Science, King Mongkut's University of Technology North Bangkok, Bangkok 10800, Thailand
* Correspondence: yupaporn.a@sci.kmutnb.ac.th

Abstract

Among various statistical process control (SPC) methods, control charts are widely employed as essential instruments for monitoring and improving process quality. This study focuses on a new modified exponentially weighted moving average (New Modified EWMA) control chart that enhances detection capability under integrated and fractionally integrated time series processes. Special attention is given to the effect of symmetry on the chart structure and performance. The proposed chart preserves a symmetric monitoring configuration, in which the two-sided design ($\text{LCL} > 0$) establishes control limits that are equally spaced around the center line, enabling balanced detection of both upward and downward shifts. Conversely, the one-sided version ($\text{LCL} = 0$) introduces a deliberate asymmetry to increase sensitivity to upward mean shifts, which is particularly useful when downward deviations are physically implausible or less critical. The efficacy of the control chart utilizing both models is assessed through Average Run Length (ARL). Herein, the explicit formula of ARL is derived and compared to the ARL obtained from the numerical integral equation (NIE) in terms of both accuracy and computational time. The efficacy of the control chart employing both models is evaluated via Average Run Length (ARL). The explicit formula for ARL is derived and compared to the ARL produced by the numerical integral equation (NIE) regarding accuracy and processing time. The accuracy of the analytical ARL expression is validated by its negligible percentage difference (%diff) in comparison to the results derived using the NIE approach and the display processing time not exceeding 3 seconds. To confirm the highest capability, the suggested method is compared to both the classic EWMA and the modified EWMA charts using evaluation metrics such as ARL and SDRL (standard deviation run length), as well as RMI (relative mean index) and PCI (performance comparison index). Finally, Its examination of US stock prices illustrates performance, employing a symmetrical two-sided control chart for the rapid detection of changes through the new modified EWMA, in contrast to standard EWMA and modified EWMA charts.

Keywords: average run length; autoregressive Fractionally Integrated; control chart; numerical integral equation; statistical process control

1. Introduction

Statistical Process Control (SPC) offers a methodical and ongoing strategy for overseeing processes through real-time data to assess whether a system maintains stability or diverges from anticipated performance. Control charts are the fundamental analytical instrument in the SPC framework, allowing practitioners to visualize process variation, swiftly detect anomalous patterns, and execute prompt corrective measures. Their adaptability has facilitated applications in several sectors, including industrial manufacturing [1], financial risk evaluation and economic management [2], environmental

 doi:10.20944/preprints202512.0072.v1

monitoring [3], and healthcare systems [4]. Modern data environments often produce intricate time-series signals. Persistence, structural changes, autocorrelation, and long-range dependence distinguish these signals. These characteristics compromise the efficacy of conventional control charts, potentially resulting in asymmetric responses, directional bias, or variable detection capabilities when applied to dynamic, real-world scenarios. These constraints are particularly significant in domains like finance and economics, where the capacity to detect both increasing and decreasing trends with equivalent precision is essential for monitoring volatility, assessing systemic risk, and identifying distinctive economic conditions.

Here, symmetry is essential for design. Symmetrical control limits enable neutrality, stability, and fair detection by responding equally to increase and decrease signals. SPC applications are more reliable in high-volatility, irregularly structured, or changing system contexts due to their symmetric behavior. Consequently, symmetry-preserving control charts provide a solid foundation for monitoring modern real-world systems across disciplines. By applying these ideas to globally influential systems like the U.S. stock market, which is a barometer for macroeconomic circumstances and a major source of financial risk and volatility, control charts become even more important. Market movements affect investor behavior, economic confidence, and indicators of systemic change. Using control charts in this context allows early identification of shifts, monitoring of uncertainty, and an unbiased perspective on price fluctuations. We can now better and faster understand U.S. financial market trends.

Control charts were initially presented by Walter A. Shewhart, [5], who suggested that current sample information may be used to differentiate between common-cause fluctuation and special-cause signals in a process. The simplicity and ease of interpretation of Shewhart charts make them ideal for spotting relatively large changes in the mean process. The cumulative sum (CUSUM) control chart, which counts variances over time, was introduced by Page [6] to make it more sensitive to moderate and minor changes. In a subsequent work, Roberts [7] created the exponentially weighted moving average (EWMA) control chart, which uses a geometrically diminishing weighting structure to enhance sensitivity to subtle or long-lasting shifts in the data. Many extensions of the EWMA framework have been proposed, building on these fundamental advancements. Patel and Divecha [8] introduced the Modified EWMA (Modified EWMA) control chart to enhance sensitivity to subtle process changes. Khan et al. [9] later verified and expanded its performance for a broader range of operating situations. Subsequently, Silpakob et al. [10] enhanced the modified EWMA chart and developed an explicit ARL formula under the AR(p) model. Its efficacy in assessing ARL surpasses that of classic modified EWMA and EWMA charts. Furthermore, recent developments in EWMA-type techniques have brought to light the significance of maintaining chart response symmetry to guarantee balanced detection of upward and downward shifts, thereby lowering directional bias and enhancing accuracy in intricate, correlated, or extremely volatile processes. Symmetric two-sided control charts are essential tools for monitoring process changes because they respond equally to increases and decreases in the signal. The EWMA, modified EWMA, and enhanced new modified EWMA were the main subjects of this investigation. Depending on the monitoring objective, some real-world applications only need one upper or lower limit, even though these charts normally include two. Even while autocorrelation exists in many real systems, conventional charts also imply data independence and uniformity, which can impair detection performance. In some circumstances, specialized or altered control charts are necessary to manage dependency and ensure accurate monitoring.

The ARIMA and ARFIMA models are widely recognized time-series frameworks because they effectively capture key real-world characteristics such as persistence, non-stationarity, and long-memory behavior, which frequently appear in financial and economic data. For the ARIMA model under financial and economic data seen in Sinu et al. [11] as well as ARIMA based on environmental series seen in Hrithik et al. [12]. Pan and Chen [13] and Rabyk and Schmid [14] have further employed these models to examine how dependence structures influence control-chart performance. ARFIMA extends the integer differencing of ARIMA through fractional differencing, allowing a more flexible representation of long-range dependence. With their broad applicability and strong forecasting performance, both models remain essential tools in time-series analysis. In this study, we focus on the ARI and ARFI classes, which are particularly suitable for data exhibiting persistence and long-memory traits features commonly observed in U.S. stock market series characterized by temporal dependence and sustained volatility. Hyung and Franses [15] demonstrated long-memory behavior using daily volatility of the S&P 500, and subsequent ARFI based applications have consistently confirmed this property in U.S. market data.

One important statistic in statistical process control is the average run length (ARL), which is the predicted amount of observations needed before a control chart indicates a state that is out of control. It consists of two parts: ARL_0, which is best when high since it represents the average run length when the process is under control, and ARL_1, which is best when low since it reflects the average run length when the process is uncontrolled and needs to be detected quickly when it shifts. In the event that a change or variation takes place in the process, the control chart needs to be able to notice it promptly and indicate whether or not it is necessary to take corrective action or conduct additional investigation. To provide evidence for this assertion, a number of strategies for calculating the ARL have been presented in the scientific literature (see [16–18]). These techniques include the Markov chain approach, Monte Carlo simulation, numerical integral equation techniques (NIE), and explicit analytical formulations.

Our primary objective in this research was to assess the efficacy and precision of the explicit formula and the Numerical Integral Equation (NIE) approach in predicting the ARL. It is worth delving further into the relative merits and shortcomings of the two methods, as prior research demonstrated that they can both produce accurate ARL estimations; however, their efficacy differs with respect to model complexity and distributional assumptions. Furthermore, comprehensive study has shown that utilizing the explicit formula can markedly decrease the computation time for determining the ARL.

According to the findings of previous studies, a significant number of scholars have presented the NIE method and established explicit formulas and effectively applied them to any field. For instance, Suriyakat and Petcharat [19] talked about ARL results they got using the NIE method for a CUSUM chart in a seasonal AR model with exogenous variables. Furthermore, Chananet and Phanyaem[20] used the NIE method on an EWMA chart based on an MA model of exogenous variables and showed the ARL performance that went with it. Using real-world economic facts, as a summary, several researchers have also published ARL results obtained using both NIE and explicit formula methods and a range of time-series models. The ARL of the CUSUM control chart was evaluated by Bualuang and Peerajit [21] and Peerajit [22] in 2023. They used the time series model as ARFI and FIMA with external factors. According to the study of Riaz et al. [23], Sunthornwat et al. [24] also came up with an explicit formula for ARL running on the HWMA control chat. These were developed under the MA with exogenous and showed better performance when compared to the CUSUM control chart. Karoon et al. [25] provided explicit ARL formulas for the double EWMA control chart in AR(p). These formulas were then used on a set of economic time series to show how well the process of finding changes works. In their study, Karoon and Areepong [26] demonstrated that the AR(p) model, which includes both trend and quadratic trend components, could derive the Average Run Length (ARL) on the adjusted modified EWMA control chart more effectively than it could on the standard EWMA and modified EWMA control charts. Recently, Karoon and Areepong [27] provided a method that explicitly uses the AR(p) model to derive ARL on the new extended EWMA control chart, which outperforms both standard EWMA and extended EWMA control charts in terms of capability.

Moreover, the literature review indicates that the general AR integrated and fractionally integrated time series models, often referred to as the ARI and ARFI models, have been incorporated into various control charts. For instance, the modified EWMA [28] in 2023 and the double modified EWMA [29] in 2025 are two examples of these control charts. Nevertheless, the new modified EWMA control chart based on ARI and ARFI models has not yet been reported to have any applications. Thus, we showcase the ARL of the new modified EWMA control chart for general ARI and ARFI models, as well as general AR integrated and fractionally integrated time series models. To complete the computation,

Preprints.org (www.preprints.org) | NOT PEER-REVIEWED | Posted: 2 December 2025 doi:10.20944/preprints202512.0072.v1

we used both the precise solution and the NIE approach. The two approaches were compared using the one- and two-sided new modified EWMA control chart for accuracy and calculation speed. Next, the conventional EWMA and modified EWMA control charts were used to compare with the proposed new modified EWMA chart based on both simulated and real-world US stock prices from the S&P 500. Furthermore, this study uses real-life data to demonstrate the change detection capabilities of the new modified EWMA control chart. It was double-checked by displaying a graph to detect changes in control charts.

2. Structures of Control Charts

In the present investigation, the EWMA control charts, the modified EWMA control charts, and the new modified EWMA control charts are all able to detect even minute and modulated alterations in the process. The charts are able to catch deviations that occur in either direction because their upper and lower control limits are positioned in a symmetrical manner around the target value. A signal is created to indicate that the process mean has begun to drift higher or lower when the observed data surpass these restrictions. This signal is generated when the data exceed these limits. This upper–lower symmetrical structure provides a balanced monitoring system that increases the sensitivity of each chart to changes in the mean of the process. In addition, the distinctive upper and lower control limit formula structures of control charts may have an impact on the capacity or sensitivity of these charts to identify changes.

2.1. The EWMA Control Chart

First, the EWMA control chart was initially published in 1959 by Roberts as the first of its kind in research on quality control [7]. Its increased performance compared to previous charts led to its widespread usage in statistical process control (SPC) for tracking and identifying small to moderate process changes. To provide an explan (1) might be used.

$$X_t = \lambda Y_t + (1-\lambda)X_{t-1}, t = 1,2,3,..., \tag{1}$$

where Y_t sequence represents observed value at time (t) with exponential white noise. λ is the exponential smoothing parameter with $0 < \lambda \leq 1$. And then, Y_{t-1} represented previously EWMA value, $Y_{t-1} = Y_0$ denotes the initial value of the EWMA statistics, and the constant value equal to $Y_0 = u$. It is necessary for the EWMA control chart (Y_t) to provide evidence of the solution of the mean $(E(Y_t))$ and the variance $(Var(Y_t))$, which may be represented as

$$E(Y_t) = \mu$$

$$Var(Y_t) = \left(\frac{\lambda}{2-\lambda}\right)\sigma^2.$$

This system provides the upper control limit (UCL) as indicated in (2) and the lower control limit (LCL) as shown in (3) to monitor the process, illustrated by the following formulas:

$$\mathrm{UCL} = \mu + W_1\sigma\sqrt{\frac{\lambda}{2-\lambda}}, \tag{2}$$

$$\mathrm{LCL} = \mu - W_1\sigma\sqrt{\frac{\lambda}{2-\lambda}}, \tag{3}$$

The width of the control limit on the EWMA control chart is denoted by the variable W_1. The EWMA stopping time (τ_{b_1}) is subsequently able to be stated as follows:

$$\tau_{b_1} = \inf\{t \geq 0 : Y_t < a_1 \text{ or } Y_t > b_1\},$$

The symbols a_1 and b_1 represent the lower control limit (abbreviated as LCL) and the upper control limit (abbreviated as UCL), respectively.

2.2. The Modified EWMA Control Chart

Second, the modified EWMA chart was initially proposed by Patel and Divecha ([8]). Thereafter, Khan et al. [9] designed it with the purpose of identifying changes in the process that range from minor to moderate magnitude. The following formula can be employed to delineate the statistics of the modified EMWA control chart. It is expressed in (4).

$$K_t = (1-\lambda)K_{t-1} + \lambda Y_t + r(Y_t - Y_{t-1}), \quad t = 1,2,3,..., \tag{4}$$

where r is the constant $(r > 0)$. K_{t-1} represented previously modified EWMA value, $K_{t-1} = K_0$ denotes the initial value of the modified EWMA statistics, and a fixed value: $K_0 = v$. The solution of the mean $(E(K_t))$ and the variance $(Var(K_t))$, which may be expressed as, must be provided by the modified EWMA control chart (K_t). To explain the modified EMWA chart's statistics, you can apply this formula.

$$E(K_t) = \mu$$

$$Var(K_t) = (\lambda + 2\lambda r + 2r^2)\sigma^2/(2-\lambda).$$

The following equations demonstrate how this system monitors the process: (5) for the upper control limit (UCL) and (6) for the lower control limit (LCL).

$$\text{UCL} = \mu + W_2\sigma\sqrt{\frac{(\lambda + 2\lambda r + 2r^2)}{2-\lambda}2-\lambda}, \tag{5}$$

$$\text{LCL} = \mu - W_2\sigma\sqrt{\frac{(\lambda + 2\lambda r + 2r^2)}{2-\lambda}2-\lambda}, \tag{6}$$

To represent the stopping time of the modified EWMA control chart, one might likely write it as follows:

$$\tau_{b_2} = \inf\{t \geq 0 : E_t < a_2 \text{ or } E_t > b_2\},$$

Further, if the value of r is equal to 0, the modified EWMA statistic is transformed into the EWMA statistic.

2.3. The New Modified EWMA Control Chart

Third, the new modified EWMA control chart was built as a modification of the modified EWMA chart. This job was accomplished by separating the chart constant r into two distinct values, $r1$ and $r2$. It is possible to characterize the statistic of the new modified EWMA control chart by utilizing the formula that is presented in (7) underneath.

$$NM_t = (1-\lambda)NM_{t-1} + (\lambda + r_1)Y_t - r_2Y_{t-1}, \quad t = 1,2,3,..., \tag{7}$$

where r_1 and r_2 are constants $(r_1 > r_2 > 0)$. NM_{t-1} represented previously new modified EWMA value, $NM_{t-1} = NM_0$ denotes the initial value of the new modified EWMA statistics, and a fixed value: $NM_0 = u$. It is important to apply the new modified EWMA control chart (NM_t) in order to offer the information that may be defined as being necessary. The solution of the mean $(E(NM_t))$ and the variance ($Var(NM_t)$) is required. Use this formula to explain the data that are displayed on the new modified EMWA chart.

$$E(NM_t) = (\lambda + r_1 - r_2)\mu/\lambda$$

$$Var(NM_t) = \frac{(\lambda + r_1)^2 + r_2^2 - 2r_2(1-\lambda)(\lambda + r_1)}{\lambda(2-\lambda)}\sigma^2.$$

Equations (8) for the upper control limit (UCL) and (9) for the lower control limit (LCL) illustrate the manner in which this system carries out the monitoring of the process.

$$\text{UCL} = (\lambda + r_1 - r_2)\frac{\mu}{\lambda} + W_3\sigma\sqrt{\frac{(\lambda + r_1)^2 + r_2^2 - 2r_2(1-\lambda)(\lambda + r_1)}{\lambda(2-\lambda)}}, \tag{8}$$

$$\text{LCL} = (\lambda + r_1 - r_2)\frac{\mu}{\lambda} - W_3\sigma\sqrt{\frac{(\lambda + r_1)^2 + r_2^2 - 2r_2(1-\lambda)(\lambda + r_1)}{\lambda(2-\lambda)}}, \tag{9}$$

The stopping time of the new modified MEWMA control chart is most likely expressed as follows:

$$\tau_h = \inf\{t \geq 0 : NM_t < l \text{ or } NM_t > h\},$$

It should be noted that the new modified EWMA statistic is transformed into the modified EWMA statistic when $r_1 = r_2 > 1$, and back into the EWMA statistic when $r_1 = r_2 = 0$.

3. Preliminaries of Integrated and Fractionally Integrated Time Series

3.1. The Autoregressive Integrated Model

The autoregressive integrated (ARI) model is a reduced ARIMA framework that retains only the autoregressive and integrated components and omits the moving average term. This standard is suitable for non-stationary time series without significant short-term shock effects that would need a moving average component. In this configuration, the noise term is supposed to be white-noise without autocorrelation. The ARI(p,d) model's operator form is shown by Equation (10), which combines the autoregressive polynomial with the differencing operator to describe the process's dynamic structure.

$$(1 - \phi_1 B - \phi_2 B^2 - \cdots - \phi_p B^p)(1-B)^d Y_t = \theta + \epsilon_t, \tag{10}$$

Expanding the backshift operator, thus

$$(1-B)^d Y_t = \theta + \phi_1 Y_{t-1} + \phi_2 Y_{t-2} + \cdots + \phi_p Y_{t-p} + \epsilon_t,$$

where θ is constant value, ϕ_i represents autoregressive coefficients, and $0 < \phi_i < 1$ at $i = 1, 2, .., p$. Moreover, the random error is shown to be ϵ_t at period time (t) which is $\epsilon_t \sim Exp(\alpha)$, The degree of differencing to achieve stationarity is denoted by d.

3.2. The Autoregressive Fractionally Integrated Model

By removing the restriction that the differencing order can only accept integer values, the Autoregressive Fractionally Integrated (ARFI) model expands the ARI framework. Due to its adaptability, the model is ideal for depicting long-memory behavior, where the correlation between observations gradually decreases with time. The autoregressive component of the ARFI model explains short-run dynamics, while the fractional differencing operator captures persistent long-term dependency. To illustrate the dynamic structure of the process, Equation (11) combines the autoregressive polynomial

 doi:10.20944/preprints202512.0072.v1

with the differencing operator to demonstrate the operator form of the ARFI(p, d) model. The ARFI (p,d) model generally looks like this:

$$(1-\phi_1 B-\phi_2 B^2-\cdots-\phi_p B^p)(1-B)^d Y_t=\theta+\epsilon_t, 0<d<1 \tag{11}$$

Therefore, by extending the backshift operator

$$(1-B)^d Y_t=\theta+\phi_1 Y_{t-1}+\phi_2 Y_{t-2}+\cdots+\phi_p Y_{t-p}+\epsilon_t, 0<d<1$$

The parameter d represents the fractional differencing order, which is non-integer and restricted to the interval $0<d<0.5$ in this context. As noted by Mcleod and Hipel [30], the fractional differencing parameter typically lies within this range to maintain the stability of the process. Under this condition, the operator $(1-B)^d$ can be expressed as an infinite binomial expansion involving successive powers of the backward-shift operator, it can be shown in (11) as follow.

$$(1-B)^d=\sum_{p=0}^{\infty}\binom{d}{p}(-B)^p=1-dB+\frac{d(d-1)}{2!}B^2-\frac{d(d-1)(d-2)}{3!}B^3+\cdots, \tag{12}$$

4. Evaluation of Average Run Length for the New Modifed EWMA Control Chart

This section formulates the ARL expressions using two complementary methodologies: the explicit analytical formulation and the Numerical Integral Equation (NIE) technique, both established inside the ARI(p,d) and ARFI(p,d) frameworks. Furthermore, it confirms the existence and uniqueness of the ARL derived from the explicit solution.

4.1. Derivation of the ARL Under the ARI(p,d) Model

ARI(p,d) is an autoregressive integrated model of order p, first studied as a particular instance of ARIMA(p,d,q) in which the moving-average component is omitted $q=0$. The current series value is presented as a linear combination of prior observations (p) plus a random error term. Let I_t be observations of the ARI (p,d) model. An elegant rewriting of the ARI(p,d) model is possible with the use of Equations (10) and (12).

$$\begin{aligned}I_t&=\theta+\epsilon_t+\left(dI_{t-1}-\frac{d(d-1)}{2!}I_{t-2}+\frac{d(d-1)(d-2)}{3!}I_{t-3}-\cdots\right)\\&\quad+\sum_{i=1}^{p}\left(\phi_i I_{t-i}-d\phi_i I_{t-(i+1)}+\frac{d(d-1)}{2!}\phi_i I_{t-(i+2)}-\frac{d(d-1)(d-2)}{3!}\phi_i I_{t-(i+3)}+\cdots\right),\end{aligned}$$

where $I_{t-1}, I_{t-2}, \ldots$ represent the initial values of ARI(p,d) model.

First, to obtain the explicit Average Run Length (ARL) for the new modified EWMA control chart under the ARI (p,d) model.

We can be adjusted by substituting Y_t from the ARI (p,d) in Equation (10) and replacing it in Equation (7). It can result in the following reformulated expression.

$$\begin{aligned}NM_t&=(1-\lambda)NM_{t-1}+(\lambda+r_1)\left[\theta+\epsilon_t+dI_{t-1}-\frac{d(d-1)}{2!}I_{t-2}+\cdots\right.\\&\quad\left.+\sum_{i=1}^{p}\left(\phi_i I_{t-i}-d\phi_i I_{t-(i+1)}+\frac{d(d-1)}{2!}\phi_i I_{t-(i+2)}-\cdots\right)\right]-r_2 I_{t-1},\end{aligned}$$

where the initial time at $t = 1$, it was set $NM_0 = u$,and $I_0 = \gamma$,
and Ω represents $dI_{t-1} - \frac{d(d-1)}{2!}I_{t-2} + \cdots + \sum_{i=1}^{p}\left(\phi_i I_{t-i} - d\phi_i I_{t-(i+1)} + \frac{d(d-1)}{2!}\phi_i I_{t-(i+2)} - \cdots\right)$.
So, Equation (7) can be rewritten as

$$NM_t = (1-\lambda)NM_{t-1} + (\lambda + r_1)(\theta + \epsilon_t + \Omega) - r_2 I_{t-1}.$$

When the process is in control, let us assume that ϵ_1 is the symmetrically control limit for NM_1. The control limits for NM_1 are defined by the interval $l < NM_1 < h$, and this symmetrically controlled limit interval is expressed using the following formulation.

$$l < (1-\lambda)u + (\lambda + r_1)(\theta + \epsilon_1 + \Omega) - r_2\gamma < h$$

Following is a revised version of the equation that was previously presented, which expresses it in terms of the variable ϵ_1:

$$l - (1-\lambda)u - (\lambda + r_1)(\theta + \Omega) + r_2\gamma < (\lambda + r_1)\epsilon_1 < h - (1-\lambda)u - (\lambda + r_1)(\theta + \Omega) + r_2\gamma$$

$$\frac{l - (1-\lambda)u + r_2\gamma}{(\lambda + r_1)} - (\theta + \Omega) < \epsilon_1 < \frac{h - (1-\lambda)u + r_2\gamma}{(\lambda + r_1)} - (\theta + \Omega)$$

Based on the Fredholm integral equation [31], which was employed to create the explicit formula for ARL, let $\vartheta(u)$ be the explicit ARL formula that is applicable to the new modified EWMA control chart while operating under the ARI (p,d) model. In the following equation, (13), it is possible to rearrange this item.

$$\vartheta(u) = 1 + \frac{1}{\lambda + r_1}\int_{\frac{l-(1-\lambda)u+r_2\gamma}{(\lambda+r_1)}-(\theta+\Omega)}^{\frac{h-(1-\lambda)u+r_2\gamma}{(\lambda+r_1)}-(\theta+\Omega)} \vartheta\Big((1-\lambda)u + (\lambda + r_1)(\theta + \epsilon_1 + \Omega) - r_2\gamma\Big) f(\epsilon_1)d\epsilon_1 \quad (13)$$

Let ρ correspond to $(1-\lambda)u + (\lambda + r_1)(\theta + \epsilon_1 + \Omega) - r_2\gamma$, and then $\frac{d\rho}{d\epsilon} = \lambda + r_1$ and solving for $d\epsilon_1$, we obtain $d\epsilon_1 = \frac{1}{\lambda + r_1}d\rho$. As a result of this, we modified the variable in (13), and the variable is now the solution in (14) in the way that follows:

$$\vartheta(u) = 1 + \frac{1}{\lambda + r_1}\int_L^H \vartheta(\rho) f\left(\frac{\rho - (1-\lambda)u + r_2\gamma}{(\lambda + r_1)} - (\theta + \Omega)\right)d\rho \quad (14)$$

The mathematical theorem known as the Fixed Point Theorem, discussed in Section 4.3, will verify the solution of the explicit ARL, which has the qualities of existence and uniqueness. It is important to take note of the fact that Equation (14) will accomplish this verification.

After we have demonstrated our existence and uniqueness, Based on the determination of $\epsilon_1 \sim Exp(\alpha)$, the solution can be found as follows:

$$\vartheta(u) = 1 + \frac{1}{\lambda + r_1}\int_l^h \vartheta(\rho)\frac{1}{\alpha}exp\left(-\frac{\rho - (1-\lambda)u + r_2\gamma}{\alpha(\lambda + r_1)} - \frac{\theta + \Omega}{\alpha}\right)d\rho$$

It can be rearranged into the following mathematical equation:

$$\vartheta(u) = 1 + \frac{1}{\alpha(\lambda + r_1)}exp\left(-\frac{\rho - (1-\lambda)u + r_2\gamma}{\alpha(\lambda + r_1)} - \frac{\theta + \Omega}{\alpha}\right)\int_l^h \vartheta(\rho)exp\left(-\frac{\rho}{\alpha(\lambda + r_1)}\right)d\rho$$

As mentioned earlier, we have defined some variables, which we will discuss further below. $C = \int_l^h \vartheta(u)C_0(u)d\rho$, $C_0(u) = exp\left(-\frac{\rho}{\alpha(\lambda+r_1)}\right)$, and $D(u) = exp\left(-\frac{\rho-(1-\lambda)u+r_2\gamma}{\alpha(\lambda+r_1)} - \frac{\theta+\Omega}{\alpha}\right)$. In order that we get the equation shown in (15):

$$\vartheta(u) = 1 + \frac{C \cdot D(u)}{\alpha(\lambda + r_1)}. \tag{15}$$

Following that, the variable C is considered.

$$C = \int_l^h \vartheta(u)C_0(u)d\rho = \frac{-\alpha(\lambda + r_1)\cdot(C_0(h) - C_0(l))}{1 + \frac{1}{\lambda}\cdot C_0(r_2\gamma)exp(\frac{\theta+\Omega}{\alpha})(C_0(h) - C_0(l))}. \tag{16}$$

Finally, (16) is replaced in (15), and the solution for the ARL of the new modified EWMA chart under the ARI(p,d) or called as $\vartheta(u)$, that is expressed in (17) as follows:

$$\vartheta(u) = 1 - \frac{\lambda \cdot C_0[(1-\lambda)u]\cdot(C_0(h) - C_0(l))}{\lambda \cdot C_0(r_2\gamma)\cdot exp(-(\theta+\Omega)) + (C_0(\lambda h) - C_0(\lambda l))}, \tag{17}$$

Consequently, the ARL of the new modified EWMA chart under the ARI(p,d) can be articulated for the symmetric two-sided control chart utilizing the formulation in (18) as follows:

$$\text{ARL}_{two-sided} = 1 - \frac{\lambda \cdot C_0[(1-\lambda)u]\cdot(C_0(h) - C_0(l))}{\lambda \cdot C_0(r_2\gamma)\cdot exp(-(\theta+\Omega)) + (C_0(\lambda h) - C_0(\lambda l))}, \tag{18}$$

While, the one-sided new modified EWMA chart under the ARI(p,d) can be expressed in (19) as follows:

$$\text{ARL}_{one-sided} = 1 - \frac{\lambda \cdot C_0[(1-\lambda)u]\cdot(C_0(h) - 1)}{\lambda \cdot C_0(r_2\gamma)\cdot exp(-(\theta+\Omega)) + (C_0(\lambda h) - 1)}. \tag{19}$$

Moreover, for ARLs based on controllable and out-of-control processes, (α) are set to α_0 and α_1. These result in a transformation of the solution $C_0(u)$ to $C_0(u) = exp\left(-\frac{\rho}{\alpha_0(\lambda+r_1)}\right)$, and $C_0(u) = exp\left(-\frac{\rho}{\alpha_1(\lambda+r_1)}\right)$ in (19), respectively.

Second, the numerical integral equation (NIE) method is used to calculate the Average Run Length (ARL) of the new modified EWMA control chart for the ARI(p,d) model. When you use the NIE method with quadrature rules, you can evaluate the ARL in a way that is both very accurate and simple to perform on the computer [18].

Let $\varrho(u)$ be the ARL of the new modified EWMA chart for the ARI(p,d) model, computed using the midpoint quadrature rule. Both the two-sided symmetric interval $[l,h]$ and the one-sided interval with $l = 0$ were used to work it out. $l \leq \zeta_1 \leq \zeta_2 \leq \cdots \leq \zeta_m \leq h$ are the parts that make it up. The quadrature rule is used to set the fixed weights as $w_j = (h-l)/m$, and then, ζ_j represents $w_j\left(j - \frac{1}{2}\right) + l$, for $j = 1, 2, ..., m$. Following the steps outlined in equation below, the quadrature rule assesses the approximation of an integral.

$$\int_l^h N(u)f(u)du \approx \sum_{j=1}^{m} w_j f(\zeta_j),$$

We compute using the quadrature rule

$$\varrho(\zeta_i) = 1 + \frac{1}{\lambda + r_1}\sum_{j=1}^{m} w_j \varrho(\zeta_j) f\left(\frac{\zeta_j - (1-\lambda)\zeta_i + r_2\gamma}{(\lambda + r_1)} - (\theta + \Omega)\right), i = 1, 2, .., n. \tag{20}$$

 doi:10.20944/preprints202512.0072.v1

The following is the matrix representation of Equation (20):

$$\varrho(\zeta_i) = 1 + \frac{1}{\lambda + r_1} \sum_{j=1}^{m} w_j \varrho(\zeta_j) f\left(\frac{\zeta_j - (1-\lambda)\zeta_1 + r_2\gamma}{(\lambda + r_1)} - (\theta + \Omega) \right)$$

$$\varrho(\zeta_i) = 1 + \frac{1}{\lambda + r_1} \sum_{j=1}^{m} w_j \varrho(\zeta_j) f\left(\frac{\zeta_j - (1-\lambda)\zeta_2 + r_2\gamma}{(\lambda + r_1)} - (\theta + \Omega) \right)$$

$$\vdots$$

$$\varrho(\zeta_i) = 1 + \frac{1}{\lambda + r_1} \sum_{j=1}^{m} w_j \varrho(\zeta_j) f\left(\frac{\zeta_j - (1-\lambda)\zeta_n + r_2\gamma}{(\lambda + r_1)} - (\theta + \Omega) \right).$$

The NIE-based ARL can be computed from the matrix equation $\mathrm{M}_{m\times 1} = (\mathrm{I}_{m\times 1} - \mathrm{R}_{m\times m})^{-1} 1_{m\times 1}$, which represents the linear system linking the transition probabilities to the expected run length [27], where $\mathrm{M}_{m\times 1} = \begin{bmatrix} \varrho(\zeta_1) \\ \varrho(\zeta_2) \\ \vdots \\ \varrho(\zeta_n) \end{bmatrix}$, $\mathrm{I}_m = diag(1, 1, .., 1)$ and $1_{m\times 1} = \begin{bmatrix} 1 \\ 1 \\ \vdots \\ 1 \end{bmatrix}$.

Changing the order of the previous equation and replacing u with ζ_i. The NIE approach obtains the numerical approximation of the integral equation for $\varrho(u)$, abbreviated as ARL, as demonstrated in the following.

$$\varrho(u) = 1 + \frac{1}{\lambda + r_1} \sum_{j=1}^{m} w_j \varrho(\zeta_j) f\left(\frac{\zeta_j - (1-\lambda)u + r_2\gamma}{(\lambda + r_1)} - (\theta + \Omega) \right). \tag{21}$$

4.2. Derivation of the ARL Under the ARFI(p,d) Model

The ARFI(p,d) model is a fractionally integrated autoregressive process characterized by the differencing parameter. It may assume non-integer values. It is regarded as a specific instance of ARFIMA(p,d,q) with $q = 0$ signifies that the present value is contingent upon historical observations and a stochastic error component. Fractional differencing engenders long-memory characteristics, rendering ARFI(p,d) more adaptable than the conventional ARI(p,d) model. Equations (11) and (12) allow for the concise reformulation of the ARFI(p,d) process in an autoregressive format for enhanced analysis.

$$F_t = \theta + \epsilon_t + \left(dF_{t-1} - \frac{d(d-1)}{2!} F_{t-2} + \frac{d(d-1)(d-2)}{3!} F_{t-3} - \cdots \right)$$
$$+ \sum_{i=1}^{p} \left(\phi_i F_{t-i} - d\phi_i F_{t-(i+1)} + \frac{d(d-1)}{2!} \phi_i F_{t-(i+2)} - \frac{d(d-1)(d-2)}{3!} \phi_i F_{t-(i+3)} + \cdots \right),$$

where $F_{t-1}, F_{t-2}, ...$ represent the initial values of ARFI(p,d) model, and $0 < d < 0.5$ refer to long-memory process.

First step: To determine the explicit Average Run Length (ARL) for the new modified EWMA control chart under the ARFI (p,d) model, one must first substitute Y_t from the ARFI (p,d) into Equation (11) and subsequently include it into Equation (7). This action may yield the subsequent reformed phrase.

$$NM_t = (1-\lambda)NM_{t-1} + (\lambda + r_1) \left[\theta + \epsilon_t + dF_{t-1} - \frac{d(d-1)}{2!} F_{t-2} + \cdots \right.$$
$$\left. + \sum_{i=1}^{p} \left(\phi_i F_{t-i} - d\phi_i F_{t-(i+1)} + \frac{d(d-1)}{2!} \phi_i F_{t-(i+2)} - \cdots \right) \right] - r_2 F_{t-1}.$$

At the beginning time $t=1$, NM_0 was designated as u, F_0 as η,
and $\mho$ is $dF_{t-1} - \frac{d(d-1)}{2!}F_{t-2} + \cdots + \sum_{i=1}^{p}\left(\phi_i F_{t-i} - d\phi_i F_{t-(i+1)} + \frac{d(d-1)}{2!}\phi_i F_{t-(i+2)} - \cdots\right)$.

Thus, Equation (7) may be reformulated as

$$NM_t = (1-\lambda)NM_{t-1} + (\lambda + r_1)(\theta + \epsilon_t + \mho) - r_2 F_{t-1}.$$

Suppose that ϵ_1 is the symmetric control limit for NM_1 when the process is in control state. This symmetric control limit range is expressed using the following formula, and the control limit for NM_1 is defined as the range $l < NM_1$ h.
All steps are expressed as in the ARI process but different parameters.

$$l < (1-\lambda)u + (\lambda + r_1)(\theta + \epsilon_1 + \mho) - r_2\eta < h$$

Here is an updated equation that was previously given, this time using the variable ϵ_1 as its expression:

$$\frac{l-(1-\lambda)u + r_2\eta}{(\lambda + r_1)} - (\theta + \mho) < \epsilon_1 < \frac{h-(1-\lambda)u + r_2\eta}{(\lambda + r_1)} - (\theta + \mho)$$

Afterwards, to derive explicit ARL formula, we will use the ARFI (p,d) model and the new modified EWMA control chart to obtain $\tilde{\varrho}(u)$. This item can be rearranged in the equation given by (22).

$$\tilde{\vartheta}(u) = 1 + \frac{1}{\lambda + r_1}\int_{\frac{l-(1-\lambda)u+r_2\eta}{(\lambda+r_1)}-(\theta+\mho)}^{\frac{h-(1-\lambda)u+r_2\eta}{(\lambda+r_1)}-(\theta+\mho)} \tilde{\vartheta}\left((1-\lambda)u + (\lambda + r_1)(\theta + \epsilon_1 + \mho) - r_2\eta\right)g(\epsilon_1)d\epsilon_1 \quad (22)$$

Let φ is $(1-\lambda)u + (\lambda + r_1)(\theta + \epsilon_1 + \mho) - r_2\eta$, and then $\frac{d\varphi}{d\epsilon} = \lambda + r_1$ and solving for $d\epsilon_1$, we obtain $d\epsilon_1 = \frac{1}{\lambda + r_1}d\varphi$. Because of this, the variable is now calculated as the answer in Equation (23) in the following manner:

$$\tilde{\vartheta}(u) = 1 + \frac{1}{\lambda + r_1}\int_{L}^{H} \tilde{\vartheta}(\varphi)g\left(\frac{\varphi-(1-\lambda)u + r_2\eta}{(\lambda + r_1)} - (\theta + \mho)\right)d\varphi \quad (23)$$

The explicit ARL's existence and uniqueness will be verified using the Fixed Point Theorem, explained in Section 4.3. Verification is made easier by solving Equation (23) after solving $\vartheta(u)$.
The solution for the ARL of the modified EWMA chart under ARFI(p,d), denoted as $\tilde{\vartheta}(u)$, is given in (24):

$$\tilde{\vartheta}(u) = 1 - \frac{\lambda \cdot C_0[(1-\lambda)u] \cdot (C_0(h) - C_0(l))}{\lambda \cdot C_0(r_2\eta) \cdot exp(-(\theta + \mho)) + (C_0(\lambda h) - C_0(\lambda l))}. \quad (24)$$

For, the NIE method is used to calculate the ARL of the two-sided new modified EWMA control chart for the ARFI(p,d) model; It can be called $\tilde{\varrho(u)}$ as equation below.

$$\tilde{\varrho}(u) = 1 + \frac{1}{\lambda + r_1}\sum_{j=1}^{m} w_j\tilde{\varrho}(\zeta_j)g\left(\frac{\zeta_j-(1-\lambda)u + r_2\eta}{(\lambda + r_1)} - (\theta + \mho)\right). \quad (25)$$

4.3. The Existence and Uniqueness of ARL

Banach's fixed-point theorem [26] proves the ARL equation's validity by revealing a unique solution for explicit formulations of the integral equation. Call any continuous function T an operation on the class of all. Example: It showed as:

$$T(\vartheta(u)) = 1 + \frac{1}{\lambda + r_1}\int_{L}^{H} \vartheta(\rho)f\left(\frac{\rho-(1-\lambda)u + r_2\gamma}{(\lambda + r_1)} - (\theta + \Omega)\right)d\rho$$

Preprints.org (www.preprints.org) | NOT PEER-REVIEWED | Posted: 2 December 2025 doi:10.20944/preprints202512.0072.v1

For a contraction operator T, Banach's fixed-point theorem states that the fixed-point theorem $T(\vartheta(u)) = \vartheta(u)$ has a unique solution. The proof of equation for ARI(p,d) running on the New modified EWMA chart is expressed as:

Proof.

$$\begin{aligned} \|T(\vartheta(u)_1) - T(\vartheta(u)_2)\|_\infty &= sup_{u\in[l,h]}|\vartheta(u)_1 - \vartheta(u)_2| \\ &= sup_{u\in[l,h]}\left|exp(D(\rho))\int_l^h((\vartheta(u)_1 - \vartheta(u)_2)\cdot C_0(\rho))d\rho\right| \\ &\le sup_{u\in[l,h]}|\|T(\vartheta(u)_1) - T(\vartheta(u)_2)\|_\infty D(u)(C_0(l) - C_0(h))| \\ &= \|T(\vartheta(u)_1) - T(\vartheta(u)_2)\|_\infty sup_{u\in[l,h]}|D(u)||C_0(l) - C_0(h)| \\ &\le s\|T(\vartheta(u)_1) - T(\vartheta(u)_2)\|_\infty \end{aligned}$$

where $s = sup_{u\in[l,h]}|D(u)||C_0(l) - C_0(h)|; 0 \le s < 1$. □

Therefore, Banach's fixed point theorem demonstrates the solution exists and is unique.

Moreover, the proof of solution based on ARFI(p,d) of the suggested control chart follows proof of the ARI(p,d) process mentioned above.

4.4. The Measure Used for Evaluating Capability

Algorithm 1 Computed the explicit ARL and arrived at the control chart coefficients to calculate the ARL on the new modified EWMA chart using the ARI and ARFI models.

Algorithm 1 The explicit ARL solution for the ARI(p,d) and ARFI(p,d) processes running on the new modified EWMA chart

Input:
- Set the coefficients values of models: θ, ϕ_i, and d.
- Set the parameters for the new modified EWMA control chart: $\lambda = 0.05, 0.15, 0.25$, $r_1 = 2$, and $r_2 = 0.1r_1, 0.4r_1, 0.8r_1$
- Set the mean: $\alpha_0 = 1$ for the in-control ARL$_0$ ($\epsilon_t \sim$ Exp(α)) and ARL$_0 = 370$
- Set the mean shifts: $\alpha_1 = (1+\delta)\alpha_0$, and $\delta = 0.0005, 0.001, 0.003, 0.005, 0.01, 0.03, 0.1, 0.3, 1$

Output:
In-control (ARL$_0$)
- Solve the ARI and ARFI models defined as I_t and F_t with exponential white noise, respectively.
- Define the initial parameters and coefficient values.
- Set the exponential white noise parameter $\alpha = \alpha_0$
- Set the lower control limit to $LCL = 0$ for one-sided charts and $LCL = 0.1, 0.5$ for symmetrically two-sided charts.
- Calculate the upper control limit. 370 is the ARL value for UCL.
Out-of-control process (ARL_1)
-Determine the mean shift $\alpha = \alpha_1 = (1+\delta)\alpha_0$, adjust shifts ($\delta$).
-Compute the ARL values of out-of-control using the explicit formula and the NIE technique.

After calculating the ARL of two methods, namely the explicit formula and the NIE algorithm:

The next step in evaluating a control chart is to look at its ARL. Here, we begin with the absolute percentage difference ($(\%diff)$), which contrasts the ARL values ($\vartheta(u)$ and $\tilde{\vartheta}(u)$) from the explicit solution with those ($\varrho(u)$ and $\tilde{\varrho}(u)$) from the NIE method for the ARI and ARFI models, respectively. It can be calculated from the equation in (26) below.

$$\%diff = \left|\frac{\text{Explicit} - \text{NIE}}{\text{Explicit}}\right| \times 100 \tag{26}$$

Preprints.org (www.preprints.org) | NOT PEER-REVIEWED | Posted: 2 December 2025 doi:10.20944/preprints202512.0072.v1

Evaluations of efficiency like SDRL are used with ARL to assess control chart capability in detecting out-of-control circumstances [32]. The SDRL for an in-control and out-of-control processes are calculated as follows:

$$\mathrm{ARL}_0 = \frac{1}{\beta}, \mathrm{SDRL}_0 = \sqrt{\frac{(1-\beta)}{\beta^2}}, \qquad \mathrm{ARL}_1 = \frac{1}{1-\nu}, \mathrm{SDRL}_1 = \sqrt{\frac{\nu}{(1-\nu)^2}} \tag{27}$$

where, the ARL_0 was set at 370, and the corresponding SDRL_0, evaluated using (27), approximates this value. Control charts with smaller ARL_1 and SDRL_1 values can detect shifts in the process mean, leading to better performance.

Moreover, the Performance Comparison Index (PCI).and the Relative Mean Index (RMI) are the main indicators used to evaluate the control charts' performance in this study. These metrics give a thorough assessment of the charts' capability to detect process alterations. One important statistic for comparison is the PCI [33], which ranks control charts according to how efficient they are in comparison to the top-performing chart. It is represented in (28) and is defined as the ratio of a particular chart's AEQL to the lowest AEQL among all charts evaluated.

$$\mathrm{PCI} = \frac{\mathrm{AEQL}}{\mathrm{AEQL}_{\text{lowest}}} \tag{28}$$

A PCI number closer to 1 indicates better capability, which allows for quicker detection of out-of-control situations with less loss.

The RMI [29] adds a primary measure of detection improvement across charts, allowing for further technique differentiation. Better process shift sensitivity with lower RMI values (around 0) boosts performance ranking. It can be calculates as in (29) below.

$$\mathrm{RMI} = \frac{1}{\Lambda} \sum_{i=1}^{\Lambda} \left| \frac{\mathrm{ARL}_1(\delta_i) - \mathrm{ARL}_{\text{lowest}}}{\mathrm{ARL}_{\text{lowest}}} \right| \tag{29}$$

where Λ is the total number of mean shift values used in the evaluation, $\mathrm{ARL}_1(\delta_i)$ is the out-of-control ARL when the process mean shift is equal to δ_i, and $\mathrm{ARL}_{\text{lowest}}$ is The lowest ARL value among all charts being compared in δ_i .

Here, the Average Extra Quadratic Loss (AEQL) [33] is utilized as a supporting statistic that is employed in the computation of PCI. The AEQL quantifies the average extra loss, which can be calculated using the following formula. As can be seen below.

$$\mathrm{AEQL} = \frac{1}{\Delta} \sum_{\delta_i=\delta_{\min}}^{\delta_{\max}} \left(\delta_i^2 \times \mathrm{ARL}_1(\delta_i) \right)$$

where, Δ is the total number of shift values from $\delta_{min}, \delta_{max} = (0.0005, 1)$, δ_i is the i^{th} mean shift value, and $\mathrm{ARL}_{(}\delta_i)$ is the out-of-control ARL at shift δ_i. Lower values of the AEQL correspond with lower values of the PCI, which is an indication that the chart is performing more effectively overall.

5. Results and Discussion

5.1. Numerical Findings

Simulation investigations on the new modified EWMA chart compare the efficiency of the NIE technique with that of the explicit formula for the $\mathrm{ARI}(p,d)$ and $\mathrm{ARFI}(p,d)$ models. As mentioned in Algorithm 1, the initial step in comparing the ARL of the two methods was to determine that $\delta = 0$ represents the in-control and δ represents the out-of-control. The NIE for ARL is created using the division point amount, or m =500. The findings are likely shown in Table 1. Please be aware that the findings derived from the two distinct approaches were calculated with the aid of a machine that was operating on Windows 10 (64-bit) and had the following specifications: an Intel Core i5-8250U CPU (1.60 GHz, up to 1.80 GHz) and 4 GB of RAM. The results demonstrate that the ARL values, derived from the ARI model with $d = 1$ and $d = 2$, can be expressed for both one-sided and symmetrically two-sided charts, with UCL values of 0, 0.1, and 0.5. While Table 2 shows the ARL results from running under the ARFI process. It is expressed to set long memory that determined different means at $d = 0.2, 0.4$. The accuracy of the results from both tables was measured using the $\%diff$, which indicated excellent accuracy, approaching 0 in all situations. Nevertheless, the explicit formula outperforms NIE in terms of performance since it calculates practically quickly due to its much lower computing time requirements. In contrast, NIE takes more time, always ranging from 2 to 3 seconds. In the future, it makes sense to compare control charts using the explicit ARL formula. The following step involves comparing the efficacy of the new modified EWMA control to the classic EWMA and modified EWMA control charts on the basis of several different situations. This comparison is performed under the ARI(p, d) and ARFI(p, d) models, with the explicit formula being used to determine the average run length (ARL). Additionally, the Standard Deviation of Working Length (SDRL) serves as a complementary metric to the ARL, helping to compare the ability to detect performance changes in the process. The results presented by the SDRL can be expressed similarly to the ARL values in all situations.

The results presented in Tables 3 and 4 illustrate a comparative analysis of the efficiencies of the EWMA, modified EWMA, and new modified EWMA charts across various parameters, with the parameter set λ for all charts being $\lambda = 0.05, 0.15, 0.25$. The lower control limit is fixed at 0, indicating a one-sided chart, and fixed at 0.5, indicating a two-sided chart; these are expressed in Tables 3 and 4, respectively. Furthermore, d is fixed at 1 and 2 under the ARI model. The new modified EWMA chart establishes constants $r_1 = 2$, $r_2 = 0.1r_1$, $0.4r_1$, and $0.8r_1$, whereas the EWMA and modified EWMA are defined with $r_1 = r = 0$ and 2, respectively. In every instance across all models, the findings demonstrated that the new modified EWMA chart exhibited reduced ARL_1 and SDRL_1 compared to the EEWMA and EWMA control charts when r_2 was held constant. Furthermore, the modified EWMA chart with a diminished r_2, specifically $r_2 = 0.1r_1$ in this study, yielded the lowest values for ARL_1 and SDRL_1. This decrease is evidenced by superior capabilities as compared to EWMA and modified EWMA charts.

Tables 5 and 6 summarize the capability results of the control charts inside the ARFI model, yielding findings congruent with those derived from the ARI model in Tables 3 and 4. In these assessments, the lower control limit (LCL) is established at 0 for the one-sided chart and at 0.5 for the two-sided chart, as indicated in Tables 5 and 6, respectively. This study fixed the differencing parameter at $d = 0.2$ and $d = 0.4$, both of which are within the fractional range $0 < d < 0.5$. These values signify long-memory behavior, indicating that previous observations have a gradually diminishing impact on the current process, leading to sustained dependency over time. The findings indicate that the new modified EWMA chart with parameters $(r_1, r_2 = 0.1r_1)$ exhibited the lowest ARL1 and SDRL1 across all scenarios, succeeded by the new modified EWMA chart with $(r_2 = 0.4r_1)$, $(r_2 = 0.8r_1)$, the modified EWMA, and the EWMA charts, respectively. The above results still indicate the new modified EWMA chart's better performance.

The PCI and RMI, which were calculated using the ARL values, were employed to illustrate that the new modified EWMA control chart performed exceptionally well, which served to corroborate the abilities of the control charts. Moreover, the new modified EWMA control chart, which uses r_2 much less than r_1, gives the ARL_1 values less than the new modified EWMA control chart, which uses r_2 near r_1. This outcome indicated that the new modified EWMA control chart, which uses r_2 much less than r_1, is an alternative chart for evaluating the efficacy of several control charts in this study's implementation of real-world datasets.

 doi:10.20944/preprints202512.0072.v1

Table 1. Comparing the accuracy of the ARL on the New Modified EWMA control chart, which are set with lower control limit both one-sided, and two-sided control charts, under the ARI(p,d) model using the explicit formula against NIE method with determined $r_1 = 2, r_2 = 0.4r_1$ and $\text{ARL}_0 = 370$.

Model	λ	θ	ϕ_1	δ	LCL	0		0.1		0.5	
					UCL	$h = 0.410315$		$h = 0.511395$		$h = 0.915714$	
					Methods	ARL	Time	ARL	Time	ARL	Time
ARI(1,1)	0.05	1	0.1	0	$\vartheta(u)$	370.21370240	< 0.01	370.08547158	< 0.01	370.17019320	< 0.01
					$\varrho(u)$	370.21369836	2.375	370.08546745	2.329	370.17018863	2.39
					$\%diff$	0.000001090		0.000001116		0.000001233	
				0.0005	$\vartheta(u)$	277.81865343	< 0.01	274.57125435	< 0.01	261.21200766	< 0.01
					$\varrho(u)$	277.81865070	2.344	274.57125160	2.421	261.21200487	2.344
					$\%diff$	0.000000982		0.000000999		0.000001069	
				0.001	$\vartheta(u)$	222.37267580	< 0.01	218.29292181	< 0.01	201.88494481	< 0.01
					$\varrho(u)$	222.37267376	2.36	218.29291978	2.359	201.88494283	2.422
					$\%diff$	0.000000917		0.000000929		0.000000979	
				0.003	$\vartheta(u)$	123.78592235	< 0.01	120.09425219	< 0.01	105.98808489	< 0.01
					$\varrho(u)$	123.78592136	2.344	120.09425122	2.359	105.98808401	2.469
					$\%diff$	0.000000798		0.000000804		0.000000829	
				0.005	$\vartheta(u)$	85.862955829	< 0.01	82.942616181	< 0.01	72.006860288	< 0.01
					$\varrho(u)$	85.862955185	2.468	82.942615555	2.406	72.006859732	2.359
					$\%diff$	0.000000749		0.000000754		0.000000773	
				0.01	$\vartheta(u)$	48.763139703	< 0.01	46.924750974	< 0.01	40.172384279	< 0.01
					$\varrho(u)$	48.763139365	2.422	46.924750647	2.39	40.172383993	2.312
					$\%diff$	0.000000694		0.000000698		0.000000711	
				0.03	$\vartheta(u)$	18.147953507	< 0.01	17.442567437	< 0.01	14.887866199	< 0.01
					$\varrho(u)$	18.147953396	2.391	17.442567330	2.343	14.887866107	2.406
					$\%diff$	0.000000612		0.000000614		0.000000621	
				0.1	$\vartheta(u)$	6.0390546030	< 0.01	5.8390012684	< 0.01	5.1138777568	< 0.01
					$\varrho(u)$	6.0390545750	2.343	5.8390012413	2.405	5.1138777332	2.312
					$\%diff$	0.000000465		0.000000464		0.000000460	
				0.3	$\vartheta(u)$	2.4930107771	< 0.01	2.4427301596	< 0.01	2.2578068241	< 0.01
					$\varrho(u)$	2.4930107712	2.391	2.4427301539	2.36	2.2578068190	2.407
					$\%diff$	0.000000237		0.000000235		0.000000227	
				1	$\vartheta(u)$	1.3456911642	< 0.01	1.3383423320	< 0.01	1.3104502905	< 0.01
					$\varrho(u)$	1.3456911636	2.359	1.3383423314	2.39	1.3104502900	2.343
					$\%diff$	0.000000043		0.000000042		0.000000041	

 doi:10.20944/preprints202512.0072.v1

Table 1. *Cont.*

Model	λ	θ	ϕ_1	ϕ_2	δ	LCL	0		0.1		0.5	
						UCL	$h = 0.248342$		$h = 0.348996$		$h = 0.751611$	
						Methods	ARL	Time	ARL	Time	ARL	Time
ARI(2,2)	0.05	1.5	0.1	0.1	0	$\vartheta(u)$	370.21370240	< 0.01	370.08547158	< 0.01	370.17019320	< 0.01
						$\varrho(u)$	370.21369836	2.375	370.08546745	2.329	370.17018863	2.39
						$\%diff$	0.000001090		0.000001116		0.000001233	
					0.0005	$\vartheta(u)$	277.81865343	< 0.01	274.57125435	< 0.01	261.21200766	< 0.01
						$\varrho(u)$	277.81865070	2.344	274.57125160	2.421	261.21200487	2.344
						$\%diff$	0.000000982		0.000000999		0.000001069	
					0.001	$\vartheta(u)$	222.37267580	< 0.01	218.29292181	< 0.01	201.88494481	< 0.01
						$\varrho(u)$	222.37267376	2.36	218.29291978	2.359	201.88494283	2.422
						$\%diff$	0.000000917		0.000000929		0.000000979	
					0.003	$\vartheta(u)$	123.78592235	< 0.01	120.09425219	< 0.01	105.98808489	< 0.01
						$\varrho(u)$	123.78592136	2.344	120.09425122	2.359	105.98808401	2.469
						$\%diff$	0.000000798		0.000000804		0.000000829	
					0.005	$\vartheta(u)$	85.862955829	< 0.01	82.942616181	< 0.01	72.006860288	< 0.01
						$\varrho(u)$	85.862955185	2.468	82.942615555	2.406	72.006859732	2.359
						$\%diff$	0.000000749		0.000000754		0.000000773	
					0.01	$\vartheta(u)$	48.763139703	< 0.01	46.924750974	< 0.01	40.172384279	< 0.01
						$\varrho(u)$	48.763139365	2.422	46.924750647	2.39	40.172383993	2.312
						$\%diff$	0.000000694		0.000000698		0.000000711	
					0.03	$\vartheta(u)$	18.147953507	< 0.01	17.442567437	< 0.01	14.887866199	< 0.01
						$\varrho(u)$	18.147953396	2.391	17.442567330	2.343	14.887866107	2.406
						$\%diff$	0.000000612		0.000000614		0.000000621	
					0.1	$\vartheta(u)$	6.0390546030	< 0.01	5.8390012684	< 0.01	5.1138777568	< 0.01
						$\varrho(u)$	6.0390545750	2.343	5.8390012413	2.405	5.1138777332	2.312
						$\%diff$	0.000000465		0.000000464		0.000000460	
					0.3	$\vartheta(u)$	2.4930107771	< 0.01	2.4427301596	< 0.01	2.2578068241	< 0.01
						$\varrho(u)$	2.4930107712	2.391	2.4427301539	2.36	2.2578068190	2.407
						$\%diff$	0.000000237		0.000000235		0.000000227	
					1	$\vartheta(u)$	1.3456911642	< 0.01	1.3383423320	< 0.01	1.3104502905	< 0.01
						$\varrho(u)$	1.3456911636	2.359	1.3383423314	2.39	1.3104502900	2.343
						$\%diff$	0.000000043		0.000000042		0.000000041	

Table 2. Comparing the accuracy of the ARL on the New Modified EWMA control chart, which are set with a lower control limit at LCL= 0 for one-sided and LCL= 0.5 for two-side control charts, under the ARFI(p,d) model using the explicit formula against NIE method with determined $r_1 = 2, r_2 = 0.4r_1$, and $\text{ARL}_0 = 370$.

λ	θ	δ	Model	ARFI$(1,d)$							
			d	$d=0.2$				$d=0.4$			
			ϕ_1	$\phi_1=0.2$		$\phi_1=-0.2$		$\phi_1=0.2$		$\phi_1=-0.2$	
			(LCL,UCL)	$(0, 0.692144)$		$(0, 0.883147)$		$(0, 0.554562)$		$(0, 0.632399)$	
			Methods	ARL	Time	ARL	Time	ARL	Time	ARL	Time
0.15	1	0	$\tilde{\vartheta}(u)$	370.05357527	< 0.01	370.11033031	< 0.01	370.14146867	< 0.01	370.07644250	< 0.01
			$\tilde{\varrho}(u)$	370.05352820	2.625	370.11025127	2.594	370.14143910	2.484	370.07640357	2.594
			$\%diff$	0.000012722		0.000021354		0.000007989		0.000010519	
		0.0005	$\tilde{\vartheta}(u)$	284.12295732	< 0.01	289.72760017	< 0.01	279.24019232	< 0.01	282.11358439	< 0.01
			$\tilde{\varrho}(u)$	284.12292850	2.501	289.72755009	2.577	279.24017477	2.547	282.11356086	2.608
			$\%diff$	0.000010143		0.000017286		0.000006283		0.000008340	
		0.001	$\tilde{\vartheta}(u)$	230.62640419	< 0.01	238.07579658	< 0.01	224.23193953	< 0.01	227.98309858	< 0.01
			$\tilde{\varrho}(u)$	230.62638450	2.485	238.07576165	2.578	224.23192776	2.438	227.98308263	2.438
			$\%diff$	0.000008537		0.000014670		0.000005250		0.000006999	
		0.003	$\tilde{\vartheta}(u)$	131.70181522	< 0.01	139.12657992	< 0.01	125.56166925	< 0.01	129.13741609	< 0.01
			$\tilde{\varrho}(u)$	131.70180790	2.469	139.12656649	2.501	125.56166499	2.532	129.13741022	2.5
			$\%diff$	0.000005560		0.000009649		0.000003392		0.000004543	
		0.005	$\tilde{\vartheta}(u)$	92.286586707	< 0.01	98.402160317	< 0.01	87.309408650	< 0.01	90.199015169	< 0.01
			$\tilde{\varrho}(u)$	92.286582677	2.5	98.402152866	2.546	87.309406322	2.562	90.199011949	2.563
			$\%diff$	0.000004367		0.000007572		0.000002667		0.000003569	
		0.01	$\tilde{\vartheta}(u)$	52.960178234	< 0.01	56.999825876	< 0.01	49.725705650	< 0.01	51.597718573	< 0.01
			$\tilde{\varrho}(u)$	52.960176561	2.484	56.999822779	2.547	49.725704684	2.516	51.597717236	2.5
			$\%diff$	0.000003159		0.000005432		0.000001943		0.000002589	
		0.03	$\tilde{\vartheta}(u)$	19.917023026	< 0.01	21.600627002	< 0.01	18.587945087	< 0.01	19.355089975	< 0.01
			$\tilde{\varrho}(u)$	19.917022617	2.452	21.600626253	2.562	18.587944848	2.562	19.355089646	2.532
			$\%diff$	0.000002056		0.000003468		0.000001285		0.000001697	
		0.1	$\tilde{\vartheta}(u)$	6.6844575161	< 0.01	7.2595651570	< 0.01	6.2336730700	< 0.01	6.4934834643	< 0.01
			$\tilde{\varrho}(u)$	6.6844574268	2.501	7.2595649948	2.515	6.2336730177	2.499	6.4934833925	2.515
			$\%diff$	0.000001336		0.000002234		0.000000839		0.000001105	
		0.3	$\tilde{\vartheta}(u)$	2.7642652085	< 0.01	2.9814943402	< 0.01	2.5952426678	< 0.01	2.6924955062	< 0.01
			$\tilde{\varrho}(u)$	2.7642651899	2.703	2.9814943060	2.485	2.5952426570	2.531	2.6924954914	2.563
			$\%diff$	0.000000673		0.000001147		0.000000415		0.000000553	
		1	$\tilde{\vartheta}(u)$	1.4500558766	< 0.01	1.5261690885	< 0.01	1.3919495203	< 0.01	1.4252423551	< 0.01
			$\tilde{\varrho}(u)$	1.4500558747	2.516	1.5261690847	2.562	1.3919495192	2.578	1.4252423536	2.499
			$\%diff$	0.000000135		0.000000245		0.000000079		0.000000108	

Table 2. *Cont.*

λ	θ	δ	Model	ARFI$(2,d)$							
			d	$d = 0.2$				$d = 0.4$			
			ϕ_1, ϕ_2	$\phi_1, \phi_2 = 0.2, 0.4$		$\phi_1, \phi_2 = 0.2, -0.4$		$\phi_1, \phi_2 = 0.2, 0.4$		$\phi_1, \phi_2 = 0.2, -0.4$	
			(LCL,UCL)	$(0.5, 0.545399)$		$(0.5, 0.572997)$		$(0.5, 0.5407292)$		$(0.5, 0.5526969)$	
			Methods	ARL	Time	ARL	Time	ARL	Time	ARL	Time
0.15	3.5	0	$\tilde{\vartheta}(u)$	370.04780163	< 0.01	370.09273890	< 0.01	370.18132219	< 0.01	370.02034117	< 0.01
			$\tilde{\varrho}(u)$	370.04780141	2.578	370.09273834	2.594	370.18132201	2.578	370.02034087	2.688
			$\%diff$	0.0000000587		0.0000001520		0.0000000479		0.0000000786	
		0.0005	$\tilde{\vartheta}(u)$	212.50418511	< 0.01	221.26755323	< 0.01	210.62842029	< 0.01	215.17853412	< 0.01
			$\tilde{\varrho}(u)$	212.50418504	2.531	221.26755301	2.594	210.62842023	2.625	215.17853401	2.532
			$\%diff$	0.0000000371		0.0000000980		0.0000000292		0.0000000499	
		0.001	$\tilde{\vartheta}(u)$	149.15102108	< 0.01	157.90603732	< 0.01	147.29195064	< 0.01	151.79886834	< 0.01
			$\tilde{\varrho}(u)$	149.15102104	2.5	157.90603720	2.563	147.29195061	2.547	151.79886828	2.594
			$\%diff$	0.0000000279		0.0000000753		0.0000000223		0.0000000379	
		0.003	$\tilde{\vartheta}(u)$	68.240909481	< 0.01	73.813635601	< 0.01	67.079011538	< 0.01	69.903749927	< 0.01
			$\tilde{\varrho}(u)$	68.240909469	2.469	73.813635568	2.531	67.079011529	2.516	69.903749911	2.625
			$\%diff$	0.0000000164		0.0000000446		0.0000000131		0.0000000224	
		0.005	$\tilde{\vartheta}(u)$	44.384810240	< 0.01	48.308784667	< 0.01	43.571806944	< 0.01	45.550726555	< 0.01
			$\tilde{\varrho}(u)$	44.384810234	2.593	48.308784650	2.501	43.571806940	2.563	45.550726547	2.578
			$\%diff$	0.0000000129		0.0000000352		0.0000000104		0.0000000177	
		0.01	$\tilde{\vartheta}(u)$	23.863597504	< 0.01	26.101197388	< 0.01	23.402632849	< 0.01	24.525948209	< 0.01
			$\tilde{\varrho}(u)$	23.863597502	2.609	26.101197381	2.516	23.402632847	2.687	24.525948205	2.624
			$\%diff$	0.0000000100		0.0000000266		0.0000000080		0.0000000136	
		0.03	$\tilde{\vartheta}(u)$	8.6920385969	< 0.01	9.5192555825	< 0.01	8.5224426837	< 0.01	8.9361439812	< 0.01
			$\tilde{\varrho}(u)$	8.6920385963	2.656	9.5192555807	2.563	8.5224426832	2.593	8.9361439803	2.5
			$\%diff$	0.0000000071		0.0000000188		0.0000000057		0.0000000096	
		0.1	$\tilde{\vartheta}(u)$	3.0947895889	< 0.01	3.3603094043	< 0.01	3.0405904182	< 0.01	3.1729361007	< 0.01
			$\tilde{\varrho}(u)$	3.0947895887	2.578	3.3603094039	2.562	3.0405904181	2.532	3.1729361005	2.484
			$\%diff$	0.0000000043		0.0000000117		0.0000000034		0.0000000059	
		0.3	$\tilde{\vartheta}(u)$	1.5317428488	< 0.01	1.6241193266	< 0.01	1.5131174218	< 0.01	1.5587407373	< 0.01
			$\tilde{\varrho}(u)$	1.5317428488	2.577	1.6241193266	2.625	1.5131174217	2.641	1.5587407373	2.594
			$\%diff$	0.0000000015		0.0000000044		0.0000000012		0.0000000021	
		1	$\tilde{\vartheta}(u)$	1.0859500052	< 0.01	1.1110193914	< 0.01	1.0811119290	< 0.01	1.0930979498	< 0.01
			$\tilde{\varrho}(u)$	1.0859500052	2.516	1.1110193914	2.531	1.0811119290	2.563	1.0930979498	2.563
			$\%diff$	0.0000000001		0.0000000005		0.0000000001		0.0000000002	

doi:10.20944/preprints202512.0072.v1

Table 3. Comparing the capabilities of one-sided control charts, all set with a lower control limit at LCL$=0$, using simulated data from the ARI(p,d) model for various shift sizes when determined $\text{ARL}_0 = 370$ with parameters defined as $\theta = 3$ and $\phi_1 = 0.3$ for $d = 1$, whereas $\theta = 2$, $\phi_1 = 0.3$, and $\phi_2 = 0.6$ for $d = 2$.

Model		ARI(1,1)									
λ	Control Chart	EWMA		Modified EWMA		New Modified EWMA					
		$r=0$		$r=2$		$r_1=2, r_2=0.1r_1$		$r_1=2, r_2=0.4r_1$		$r_1=2, r_2=0.8r_1$	
0.05	UCL	$b_1 = 1.894 \times 10^{-9}$		$b_2 = 0.099307$		$h = 0.04124$		$h = 0.0552722$		$h = 0.081685$	
	δ	ARL_1	SDRL_1	ARL_1	SDRL_1	ARL_1	SDRL_1	ARL_1	SDRL_1	ARL_1	SDRL_1
	0.0005	365.733	365.233	250.316	249.815	235.141	234.640	239.884	239.383	247.094	246.593
	0.001	361.389	360.889	189.148	188.647	172.243	171.742	177.503	177.002	185.316	184.815
	0.003	344.563	344.063	95.773	95.272	83.332	82.831	87.125	86.623	92.776	92.275
	0.005	328.584	328.084	64.208	63.706	55.047	54.544	57.816	57.314	61.964	61.462
	0.01	292.047	291.547	35.320	34.816	29.889	29.385	31.518	31.014	33.971	33.467
	0.03	184.405	183.904	12.839	12.329	10.779	10.267	11.393	10.881	12.322	11.811
	0.1	42.469	41.966	4.287	3.754	3.627	3.087	3.823	3.285	4.120	3.585
	0.3	2.407	1.840	1.865	1.270	1.641	1.025	1.706	1.098	1.807	1.208
	1	1.002	0.043	1.154	0.421	1.096	0.324	1.112	0.353	1.138	0.397
	PCI	1.429		1.068		1		1.019		1.050	
	RMI	5.081		0.136		0		0.041		0.102	
0.15	UCL	$b_1 = 0.001545$		$b_2 = 0.099783$		$h = 0.043111$		$h = 0.0570161$		$h = 0.0827931$	
	δ	ARL_1	SDRL_1	ARL_1	SDRL_1	ARL_1	SDRL_1	ARL_1	SDRL_1	ARL_1	SDRL_1
	0.001	367.044	366.544	244.163	243.662	229.436	228.935	233.929	233.428	240.632	240.131
	0.003	363.947	363.447	182.223	181.722	166.139	165.638	171.083	170.582	178.352	177.851
	0.005	351.907	351.407	90.590	90.089	79.127	78.625	82.610	82.108	87.776	87.274
	0.01	340.402	339.902	60.382	59.880	52.031	51.528	54.553	54.051	58.315	57.813
	0.03	313.783	313.283	33.065	32.561	28.162	27.658	29.634	29.130	31.843	31.339
	0.05	231.361	230.860	12.022	11.511	10.175	9.662	10.726	10.214	11.558	11.047
	0.1	95.726	95.225	4.063	3.528	3.472	2.929	3.647	3.107	3.914	3.377
	0.5	17.158	16.650	1.810	1.211	1.608	0.989	1.667	1.055	1.758	1.155
	1	1.671	1.059	1.145	0.408	1.092	0.317	1.107	0.344	1.131	0.385
	PCI	3.440		1.062		1		1.018		1.046	
	RMI	8.826		0.130		0		0.039		0.097	

Preprints.org (www.preprints.org) | NOT PEER-REVIEWED | Posted: 2 December 2025 doi:10.20944/preprints202512.0072.v1

Table 3. *Cont.*

Model		ARI(2,2)									
0.25	UCL	$b_1 = 0.004354$		$b_2 = 0.100428$		$h = 0.044985$		$h = 0.058778$		$h = 0.083994$	
	δ	ARL_1	$SDRL_1$	ARL_1	$SDRL_1$	ARL_1	$SDRL_1$	ARL_1	$SDRL_1$	ARL_1	$SDRL_1$
	0.001	353.142	352.642	238.594	238.093	223.815	223.314	228.460	227.959	235.332	234.831
	0.003	336.942	336.442	176.015	175.514	160.440	159.939	165.294	164.793	172.415	171.914
	0.005	284.238	283.738	86.064	85.562	75.399	74.897	78.657	78.155	83.481	82.980
	0.01	245.239	244.738	57.073	56.571	49.394	48.891	51.722	51.220	55.190	54.688
	0.03	181.263	180.762	31.134	30.629	26.669	26.165	28.014	27.510	30.027	29.523
	0.05	84.274	83.772	11.326	10.815	9.656	9.142	10.156	9.643	10.909	10.397
	0.1	23.775	23.269	3.873	3.335	3.338	2.794	3.497	2.955	3.738	3.199
	0.5	5.087	4.560	1.763	1.160	1.580	0.957	1.634	1.018	1.717	1.109
	1	1.307	0.633	1.138	0.396	1.089	0.312	1.103	0.337	1.125	0.375
PCI		1.647		1.057		1		1.016		1.042	
RMI		3.387		0.125		0		0.038		0.094	
λ	Control Chart	EWMA		Modified EWMA		New Modified EWMA					
		$r = 0$		$r = 2$		$r_1 = 2, r_2 = 0.1r_1$		$r_1 = 2, r_2 = 0.4r_1$		$r_1 = 2, r_2 = 0.8r_1$	
0.05	UCL	$b_1 = 5.15 \times 10^{-9}$		$b_2 = 0.270552$		$h = 0.112206$		$h = 0.150434$		$h = 0.222452$	
	δ	ARL_1	$SDRL_1$	ARL_1	$SDRL_1$	ARL_1	$SDRL_1$	ARL_1	$SDRL_1$	ARL_1	$SDRL_1$
	0.0005	366.027	365.527	269.483	268.983	252.544	252.044	258.152	257.652	265.595	265.095
	0.001	361.859	361.359	211.882	211.381	191.712	191.211	198.178	197.677	207.141	206.640
	0.003	345.697	345.197	114.348	113.847	97.759	97.258	102.843	102.342	110.284	109.783
	0.005	330.318	329.818	78.398	77.897	65.695	65.193	69.529	69.027	75.240	74.738
	0.01	295.033	294.533	44.027	43.524	36.215	35.712	38.539	38.036	42.057	41.554
	0.03	189.883	189.382	16.243	15.735	13.184	12.674	14.082	13.573	15.462	14.953
	0.1	46.429	45.926	5.402	4.876	4.399	3.866	4.691	4.161	5.143	4.616
	0.3	2.772	2.216	2.260	1.687	1.903	1.311	2.006	1.420	2.167	1.590
	1	1.003	0.056	1.271	0.586	1.164	0.438	1.194	0.481	1.242	0.548
PCI		1.380		1.109		1		1.030		1.080	
RMI		4.258		0.165		0		0.049		0.124	

Table 3. *Cont.*

Model		ARI(2,2)									
0.15	UCL	$b_1 = 0.00422$		$b_2 = 0.272913$		$h = 0.117498$		$h = 0.155531$		$h = 0.226207$	
	δ	ARL_1	$SDRL_1$	ARL_1	$SDRL_1$	ARL_1	$SDRL_1$	ARL_1	$SDRL_1$	ARL_1	$SDRL_1$
	0.001	367.601	367.101	264.029	263.529	247.348	246.847	252.816	252.316	260.310	259.810
	0.003	364.905	364.405	205.289	204.788	185.743	185.242	191.962	191.461	200.746	200.245
	0.005	354.380	353.880	108.770	108.269	93.191	92.689	97.945	97.444	104.959	104.458
	0.01	344.258	343.758	74.094	73.592	62.302	61.800	65.850	65.348	71.162	70.660
	0.03	320.589	320.089	41.380	40.877	34.208	33.704	36.337	35.834	39.570	39.067
	0.05	244.904	244.403	15.242	14.733	12.457	11.947	13.275	12.765	14.530	14.021
	0.1	110.372	109.871	5.115	4.588	4.204	3.670	4.469	3.938	4.880	4.352
	0.5	22.489	21.983	2.183	1.607	1.859	1.264	1.952	1.363	2.099	1.518
	1	2.136	1.558	1.257	0.568	1.159	0.429	1.186	0.470	1.230	0.532
PCI		3.990		1.101		1		1.028		1.074	
RMI		8.112		0.160		0		0.048		0.120	
0.25	UCL	$b_1 = 0.011886$		$b_2 = 0.275681$		$h = 0.122817$		$h = 0.160691$		$h = 0.230195$	
	δ	ARL_1	$SDRL_1$	ARL_1	$SDRL_1$	ARL_1	$SDRL_1$	ARL_1	$SDRL_1$	ARL_1	$SDRL_1$
	0.001	355.884	355.384	259.081	258.581	242.500	241.999	247.880	247.379	255.319	254.819
	0.003	342.398	341.898	199.346	198.845	180.307	179.806	186.322	185.821	194.872	194.371
	0.005	296.965	296.465	103.869	103.368	89.168	88.667	93.638	93.136	100.254	99.753
	0.01	261.719	261.219	70.353	69.851	59.347	58.845	62.650	62.148	67.606	67.105
	0.03	200.646	200.145	39.103	38.600	32.476	31.972	34.441	33.937	37.427	36.924
	0.05	99.380	98.879	14.388	13.878	11.835	11.324	12.584	12.074	13.735	13.225
	0.1	29.866	29.361	4.870	4.341	4.037	3.501	4.280	3.747	4.656	4.125
	0.5	6.722	6.202	2.118	1.539	1.821	1.222	1.906	1.314	2.040	1.457
	1	1.528	0.898	1.244	0.552	1.154	0.422	1.179	0.460	1.220	0.518
PCI		1.855		1.094		1		1.026		1.069	
RMI		3.233		0.155		0		0.046		0.116	

doi:10.20944/preprints202512.0072.v1

Table 4. Comparing the capabilities of two-sided control charts, all set with a lower control limit at LCL$=0.5$, using simulated data from the ARI(p,d) model for various shift sizes when determined $\text{ARL}_0 = 370$ with parameters defined as $\theta = 3$ and $\phi_1 = 0.3$ for $d = 1$, whereas $\theta = 2$, $\phi_1 = 0.3$, and $\phi_2 = 0.6$ for $d = 2$.

Model		ARI(1,2)									
λ	Control Chart	EWMA		Modified EWMA		New Modified EWMA					
		$r=0$		$r=2$		$r_1=2, r_2=0.1r_1$		$r_1=2, r_2=0.4r_1$		$r_1=2, r_2=0.8r_1$	
0.05	UCL	$b_1=0.5000406$		$b_2=0.600615$		$h=0.541783$		$h=0.556$		$h=0.58276$	
	δ	ARL_1	SDRL_1	ARL_1	SDRL_1	ARL_1	SDRL_1	ARL_1	SDRL_1	ARL_1	SDRL_1
	0.0005	367.421	366.921	231.473	230.972	215.082	214.581	220.133	219.632	227.540	227.039
	0.001	364.846	364.346	168.337	167.836	151.573	151.072	156.732	156.231	164.286	163.785
	0.003	354.751	354.251	80.707	80.205	69.696	69.195	73.031	72.529	77.990	77.488
	0.005	344.974	344.474	53.216	52.714	45.389	44.886	47.745	47.242	51.270	50.768
	0.01	321.851	321.351	28.920	28.415	24.419	23.913	25.765	25.260	27.793	27.288
	0.03	245.510	245.009	10.554	10.041	8.879	8.364	9.377	8.863	10.132	9.619
	0.1	102.945	102.444	3.679	3.140	3.140	2.592	3.299	2.754	3.542	3.001
	0.3	14.882	14.373	1.728	1.121	1.539	0.911	1.594	0.973	1.679	1.068
	1	1.271	0.586	1.138	0.396	1.086	0.305	1.100	0.332	1.124	0.373
PCI		3.079		1.061		1		1.017		1.045	
RMI		10.252		0.137		0		0.041		0.103	
0.15	UCL	$b_1=0.504342$		$b_2=0.603412$		$h=0.5446753$		$h=0.5590865$		$h=0.5858021$	
	δ	ARL_1	SDRL_1	ARL_1	SDRL_1	ARL_1	SDRL_1	ARL_1	SDRL_1	ARL_1	SDRL_1
	0.001	351.662	351.162	228.321	227.820	212.227	211.726	217.307	216.806	224.374	223.873
	0.003	334.729	334.229	165.036	164.535	148.874	148.373	153.907	153.406	161.085	160.584
	0.005	280.241	279.741	78.477	77.975	68.067	67.565	71.236	70.734	75.900	75.399
	0.01	240.503	240.002	51.623	51.121	44.263	43.760	46.487	45.984	49.792	49.289
	0.03	176.353	175.852	28.008	27.503	23.794	23.289	25.059	24.554	26.954	26.449
	0.05	81.435	80.933	10.229	9.716	8.667	8.151	9.133	8.618	9.836	9.323
	0.1	23.385	22.880	3.590	3.049	3.087	2.538	3.236	2.690	3.463	2.920
	0.5	5.280	4.753	1.705	1.097	1.529	0.899	1.581	0.958	1.660	1.047
	1	1.372	0.714	1.134	0.390	1.085	0.304	1.099	0.330	1.121	0.369
PCI		1.723		1.057		1		1.016		1.042	
RMI		3.729		0.132		0		0.040		0.099	

doi:10.20944/preprints202512.0072.v1

Table 4. *Cont.*

Model	ARI(2,1)										
	UCL	$b_1 = 0.5074878$		$b_2 = 0.60626$		$h = 0.547589$		$h = 0.5621833$		$h = 0.588867$	
	δ	ARL_1	$SDRL_1$	ARL_1	$SDRL_1$	ARL_1	$SDRL_1$	ARL_1	$SDRL_1$	ARL_1	$SDRL_1$
0.25	0.001	311.216	310.716	225.241	224.740	209.829	209.328	214.758	214.257	221.809	221.308
	0.003	268.299	267.799	161.952	161.451	146.541	146.040	151.374	150.873	158.363	157.862
	0.005	172.642	172.141	76.472	75.970	66.637	66.135	69.641	69.139	74.080	73.578
	0.01	127.031	126.530	50.205	49.702	43.273	42.770	45.373	44.871	48.499	47.996
	0.03	76.136	75.634	27.202	26.697	23.245	22.739	24.436	23.930	26.219	25.714
	0.05	28.539	28.035	9.944	9.431	8.479	7.964	8.918	8.403	9.577	9.063
	0.1	8.307	7.791	3.511	2.969	3.040	2.490	3.180	2.633	3.393	2.849
	0.5	2.614	2.054	1.685	1.075	1.520	0.889	1.569	0.945	1.643	1.028
	1	1.198	0.487	1.131	0.385	1.085	0.303	1.098	0.328	1.119	0.365
PCI		1.230		1.054		1		1.015		1.040	
RMI		1.338		0.126		0		0.038		0.095	
λ	Control Chart	EWMA		Modified EWMA		New Modified EWMA					
		$r = 0$		$r = 2$		$r_1 = 2, r_2 = 0.1r_1$		$r_1 = 2, r_2 = 0.4r_1$		$r_1 = 2, r_2 = 0.8r_1$	
	UCL	$b_1 = 0.5001105$		$b_2 = 0.774113$		$h = 0.613684$		$h = 0.652414$		$h = 0.72538$	
	δ	ARL_1	$SDRL_1$	ARL_1	$SDRL_1$	ARL_1	$SDRL_1$	ARL_1	$SDRL_1$	ARL_1	$SDRL_1$
0.05	0.0005	367.823	367.323	252.081	251.581	233.930	233.429	239.577	239.076	247.786	247.285
	0.001	365.432	364.932	191.141	190.640	170.925	170.424	177.177	176.676	186.290	185.789
	0.003	356.047	355.547	97.377	96.876	82.483	81.981	86.975	86.474	93.688	93.187
	0.005	346.939	346.439	65.476	64.974	54.497	53.995	57.775	57.273	62.725	62.223
	0.01	325.319	324.819	36.188	35.685	29.666	29.161	31.594	31.090	34.536	34.032
	0.03	253.067	252.567	13.329	12.819	10.834	10.322	11.566	11.054	12.691	12.181
	0.1	112.911	112.410	4.592	4.061	3.770	3.232	4.009	3.473	4.380	3.847
	0.3	18.540	18.033	2.061	1.479	1.760	1.157	1.846	1.250	1.982	1.395
	1	1.447	0.805	1.243	0.550	1.148	0.412	1.174	0.452	1.217	0.514
PCI		3.325		1.099		1		1.027		1.072	
RMI		9.051		0.167		0		0.049		0.124	

doi:10.20944/preprints202512.0072.v1

Table 4. *Cont.*

Model		ARI(2,1)									
0.15	UCL	$b_1 = 0.511858$		$b_2 = 0.782894$		$h = 0.621773$		$h = 0.661197$		$h = 0.734467$	
	δ	ARL_1	$SDRL_1$	ARL_1	$SDRL_1$	ARL_1	$SDRL_1$	ARL_1	$SDRL_1$	ARL_1	$SDRL_1$
	0.001	355.341	354.841	249.393	248.892	231.429	230.928	237.298	236.797	245.353	244.852
	0.003	341.423	340.923	188.144	187.643	168.400	167.899	174.646	174.145	183.515	183.014
	0.005	294.845	294.345	95.120	94.619	80.809	80.307	85.153	84.652	91.596	91.095
	0.01	259.037	258.537	63.802	63.300	53.306	52.803	56.450	55.948	61.179	60.677
	0.03	197.644	197.143	35.195	34.691	28.987	28.483	30.825	30.321	33.623	33.119
	0.05	97.590	97.089	12.963	12.452	10.597	10.085	11.291	10.779	12.357	11.847
	0.1	29.884	29.379	4.486	3.955	3.709	3.170	3.936	3.399	4.286	3.753
	0.5	7.092	6.573	2.032	1.448	1.748	1.144	1.830	1.232	1.958	1.370
	1	1.647	1.032	1.237	0.542	1.147	0.411	1.172	0.449	1.213	0.508
PCI		1.992		1.094		1		1.026		1.069	
RMI		3.627		0.162		0		0.048		0.121	
0.25	UCL	$b_1 = 0.520491$		$b_2 = 0.791854$		$h = 0.629959$		$h = 0.670055$		$h = 0.743664$	
	δ	ARL_1	$SDRL_1$	ARL_1	$SDRL_1$	ARL_1	$SDRL_1$	ARL_1	$SDRL_1$	ARL_1	$SDRL_1$
	0.001	321.870	321.370	247.050	246.549	229.559	229.058	234.997	234.496	243.038	242.537
	0.003	284.602	284.102	185.510	185.009	166.348	165.847	172.254	171.753	180.965	180.464
	0.005	194.282	193.781	93.142	92.640	79.380	78.878	83.516	83.014	89.735	89.234
	0.01	147.265	146.764	62.337	61.835	52.280	51.777	55.274	54.771	59.815	59.312
	0.03	91.400	90.898	34.328	33.824	28.399	27.895	30.148	29.644	32.823	32.319
	0.05	35.563	35.059	12.644	12.133	10.391	9.879	11.051	10.539	12.066	11.556
	0.1	10.613	10.101	4.395	3.863	3.656	3.116	3.871	3.334	4.204	3.670
	0.5	3.317	2.772	2.007	1.422	1.737	1.132	1.815	1.216	1.937	1.347
	1	1.346	0.682	1.233	0.535	1.147	0.410	1.170	0.447	1.209	0.503
PCI		1.328		1.089		1		1.025		1.065	
RMI		1.334		0.157		0		0.046		0.118	

Table 5. Comparing the capabilities of one-sided control charts, all set with a lower control limit at LCL$=0$, using simulated data from the ARFI$(1,d)$ model for various shift sizes when determined ARL$_0 = 370$ with parameters defined as $\theta = 2.5$ and $\phi_1 = 0.5$, $d = 0.2$, and 0.4 .

Model	ARFI(1,0.2)										
λ	Control Chart	EWMA		Modified EWMA		New Modified EWMA					
		$r=0$		$r=2$		$r_1=2, r_2=0.1r_1$		$r_1=2, r_2=0.4r_1$		$r_1=2, r_2=0.8r_1$	
0.05	UCL	$b_1 = 4.2\times10^{-9}$		$b_2 = 0.22053$		$h=0.091495$		$h=0.122655$		$h=0.181343$	
	δ	ARL$_1$	SDRL$_1$	ARL$_1$	SDRL$_1$	ARL$_1$	SDRL$_1$	ARL$_1$	SDRL$_1$	ARL$_1$	SDRL$_1$
	0.0005	365.942	365.442	265.801	265.301	248.911	248.410	254.246	253.746	261.658	261.158
	0.001	361.739	361.239	207.162	206.661	187.499	186.998	193.651	193.150	202.378	201.877
	0.003	345.443	344.943	110.174	109.673	94.490	93.988	99.261	98.759	106.291	105.790
	0.005	329.942	329.442	75.134	74.633	63.247	62.745	66.822	66.320	72.163	71.661
	0.01	294.403	293.903	41.982	41.479	34.741	34.238	36.895	36.392	40.155	39.651
	0.03	188.741	188.240	15.430	14.921	12.617	12.107	13.446	12.936	14.713	14.204
	0.1	45.590	45.087	5.133	4.605	4.216	3.682	4.484	3.952	4.897	4.369
	0.3	2.690	2.133	2.163	1.586	1.840	1.243	1.933	1.343	2.079	1.497
	1	1.003	0.053	1.241	0.546	1.147	0.411	1.173	0.450	1.215	0.511
PCI		1.393		1.099		1		1.028		1.072	
RMI		4.428		0.159		0		0.047		0.119	
0.15	UCL	$b_1 = 0.003439$		$b_2 = 0.2222$		$h=0.095762$		$h=0.126727$		$h=0.184228$	
	δ	ARL$_1$	SDRL$_1$	ARL$_1$	SDRL$_1$	ARL$_1$	SDRL$_1$	ARL$_1$	SDRL$_1$	ARL$_1$	SDRL$_1$
	0.001	367.919	367.419	260.213	259.713	243.514	243.013	248.714	248.213	256.077	255.577
	0.003	365.136	364.636	200.472	199.971	181.433	180.932	187.336	186.835	195.806	195.305
	0.005	354.284	353.784	104.648	104.147	89.975	89.473	94.420	93.919	101.001	100.500
	0.01	343.862	343.362	70.912	70.410	59.923	59.421	63.220	62.718	68.158	67.656
	0.03	319.544	319.044	39.411	38.907	32.791	32.287	34.758	34.254	37.737	37.234
	0.05	242.303	241.802	14.466	13.957	11.917	11.406	12.668	12.158	13.817	13.308
	0.1	107.241	106.740	4.859	4.330	4.029	3.494	4.272	3.739	4.646	4.116
	0.5	21.264	20.757	2.091	1.510	1.798	1.198	1.883	1.289	2.015	1.430
	1	2.020	1.435	1.228	0.529	1.142	0.403	1.166	0.440	1.205	0.497
PCI		3.871		1.091		1		1.026		1.067	
RMI		8.276		0.153		0		0.045		0.114	

doi:10.20944/preprints202512.0072.v1

Table 5. *Cont.*

Model	ARFI(1,0.4)										
	UCL	$b_1 = 0.009682$		$b_2 = 0.224211$		$h = 0.100047$		$h = 0.130847$		$h = 0.187306$	
	δ	ARL_1	$SDRL_1$	ARL_1	$SDRL_1$	ARL_1	$SDRL_1$	ARL_1	$SDRL_1$	ARL_1	$SDRL_1$
0.25	0.001	354.944	354.444	254.761	254.261	238.636	238.135	243.715	243.214	250.913	250.413
	0.003	340.928	340.428	194.223	193.722	175.998	175.497	181.675	181.174	189.835	189.334
	0.005	294.040	293.540	99.741	99.240	86.022	85.520	90.182	89.681	96.348	95.847
	0.01	258.014	257.514	67.220	66.718	57.038	56.536	60.095	59.593	64.676	64.174
	0.03	196.296	195.795	37.193	36.689	31.111	30.607	32.919	32.415	35.658	35.154
	0.05	95.907	95.406	13.644	13.135	11.317	10.806	12.004	11.493	13.052	12.542
	0.1	28.430	27.925	4.626	4.095	3.870	3.332	4.091	3.556	4.432	3.900
	0.5	6.328	5.806	2.030	1.446	1.762	1.159	1.840	1.243	1.960	1.372
	1	1.472	0.833	1.217	0.514	1.138	0.396	1.160	0.431	1.196	0.484
	PCI	1.807		1.084		1.000		1.024		1.062	
	RMI	3.265		0.147		0.000		0.044		0.110	
λ	Control Chart	EWMA		Modified EWMA		New Modified EWMA					
		$r = 0$		$r = 2$		$r_1 = 2, r_2 = 0.1r_1$		$r_1 = 2, r_2 = 0.4r_1$		$r_1 = 2, r_2 = 0.8r_1$	
	UCL	$b_1 = 3.67 \times 10^{-9}$		$b_2 = 0.192517$		$h = 0.079891$		$h = 0.107093$		$h = 0.158319$	
	δ	ARL_1	$SDRL_1$	ARL_1	$SDRL_1$	ARL_1	$SDRL_1$	ARL_1	$SDRL_1$	ARL_1	$SDRL_1$
0.05	0.0005	366.130	365.630	262.849	262.349	246.728	246.227	251.808	251.308	259.022	258.522
	0.001	361.900	361.400	203.783	203.282	184.886	184.385	190.794	190.293	199.265	198.764
	0.003	345.504	345.004	107.443	106.942	92.445	91.944	97.010	96.509	103.754	103.253
	0.005	329.912	329.412	73.045	72.543	61.717	61.215	65.128	64.626	70.227	69.725
	0.01	294.180	293.680	40.697	40.194	33.823	33.319	35.871	35.367	38.968	38.465
	0.03	188.111	187.610	14.926	14.417	12.265	11.755	13.051	12.541	14.250	13.741
	0.1	45.069	44.567	4.967	4.439	4.102	3.567	4.355	3.823	4.745	4.216
	0.3	2.639	2.080	2.103	1.523	1.801	1.201	1.888	1.295	2.025	1.441
	1	1.003	0.051	1.223	0.522	1.136	0.394	1.160	0.431	1.199	0.489
	PCI	1.402		1.092		1		1.026		1.068	
	RMI	4.544		0.154		0		0.046		0.115	

doi:10.20944/preprints202512.0072.v1

Table 5. *Cont.*

Model		ARFI(1,0.4)									
	UCL	$b_1 = 0.002999$		$b_2 = 0.193851$		$h = 0.083593$		$h = 0.110608$		$h = 0.160752$	
	δ	ARL_1	$SDRL_1$	ARL_1	$SDRL_1$	ARL_1	$SDRL_1$	ARL_1	$SDRL_1$	ARL_1	$SDRL_1$
0.15	0.001	367.307	366.807	257.201	256.701	241.085	240.584	246.371	245.870	253.315	252.815
	0.003	364.475	363.975	197.063	196.562	178.698	178.197	184.545	184.044	192.626	192.125
	0.005	353.439	352.939	101.972	101.471	87.953	87.452	92.243	91.742	98.509	98.007
	0.01	342.848	342.348	68.888	68.387	58.434	57.932	61.593	61.091	66.281	65.779
	0.03	318.172	317.672	38.180	37.676	31.908	31.404	33.781	33.277	36.600	36.097
	0.05	240.128	239.627	13.988	13.479	11.582	11.071	12.293	11.783	13.377	12.867
	0.1	105.062	104.561	4.702	4.172	3.921	3.385	4.151	3.616	4.503	3.971
	0.5	20.471	19.965	2.035	1.451	1.761	1.158	1.840	1.244	1.964	1.376
	1	1.948	1.359	1.211	0.505	1.132	0.386	1.154	0.421	1.190	0.475
PCI		3.791		1.085		1		1.024		1.063	
RMI		8.366		0.149		0		0.045		0.111	
	UCL	$b_1 = 0.00845$		$b_2 = 0.195489$		$h = 0.0873081$		$h = 0.114162$		$h = 0.163356$	
	δ	ARL_1	$SDRL_1$	ARL_1	$SDRL_1$	ARL_1	$SDRL_1$	ARL_1	$SDRL_1$	ARL_1	$SDRL_1$
0.25	0.001	355.059	354.559	251.801	251.301	235.735	235.234	241.022	240.521	248.281	247.780
	0.003	340.637	340.137	190.853	190.352	173.024	172.523	178.702	178.201	186.738	186.237
	0.005	292.629	292.129	97.134	96.633	83.991	83.490	88.012	87.510	93.933	93.432
	0.01	255.992	255.492	65.264	64.762	55.572	55.070	58.500	57.998	62.867	62.365
	0.03	193.725	193.224	36.012	35.508	30.256	29.751	31.975	31.471	34.569	34.066
	0.05	93.774	93.273	13.188	12.679	10.996	10.484	11.645	11.134	12.633	12.123
	0.1	27.544	27.039	4.477	3.945	3.766	3.228	3.975	3.439	4.296	3.763
	0.5	6.086	5.563	1.976	1.389	1.726	1.120	1.799	1.199	1.912	1.320
	1	1.438	0.794	1.200	0.491	1.128	0.380	1.148	0.413	1.181	0.462
PCI		1.777		1.079		1		1.022		1.058	
RMI		3.290		0.143		0		0.043		0.108	

Preprints.org (www.preprints.org) | NOT PEER-REVIEWED | Posted: 2 December 2025 doi:10.20944/preprints202512.0072.v1

Table 6. Comparing the capabilities of two-sided control charts, all set with a lower control limit at LCL$=0.5$, using simulated data from the ARFI$(2,d)$ model for various shift sizes when determined ARL$_0=370$ with parameters defined as $\theta=1.5$, $\phi_1=0.5$, and $\phi_2=0.7$, whereas $d=0.2$, and 0.4 .

Model	ARFI(2,0.2)										
λ	Control Chart	EWMA		Modified EWMA		New Modified EWMA					
		$r=0$		$r=2$		$r_1=2, r_2=0.1r_1$		$r_1=2, r_2=0.4r_1$		$r_1=2, r_2=0.8r_1$	
0.05	UCL	$b_1=0.500162$		$b_2=0.9021$		$h=0.666603$		$h=0.723415$		$h=0.830517$	
	δ	ARL$_1$	SDRL$_1$	ARL$_1$	SDRL$_1$	ARL$_1$	SDRL$_1$	ARL$_1$	SDRL$_1$	ARL$_1$	SDRL$_1$
	0.0005	368.108	367.608	260.444	259.944	241.398	240.897	247.572	247.071	256.144	255.644
	0.001	365.787	365.287	200.981	200.480	179.183	178.682	186.065	185.564	195.871	195.370
	0.003	356.671	356.171	105.252	104.751	88.430	87.928	93.525	93.024	101.105	100.604
	0.005	347.816	347.316	71.445	70.943	58.842	58.340	62.605	62.103	68.286	67.784
	0.01	326.771	326.271	39.827	39.324	32.225	31.721	34.465	33.961	37.893	37.390
	0.03	256.106	255.606	14.752	14.243	11.806	11.295	12.664	12.153	13.993	13.483
	0.1	117.014	116.513	5.068	4.541	4.088	3.553	4.371	3.838	4.813	4.284
	0.3	20.188	19.682	2.240	1.667	1.875	1.281	1.979	1.392	2.144	1.566
	1	1.542	0.914	1.304	0.630	1.183	0.465	1.216	0.512	1.271	0.587
PCI		3.411		1.119		1		1.033		1.087	
RMI		8.560		0.181		0		0.053		0.135	
0.15	UCL	$b_1=0.517425$		$b_2=0.916255$		$h=0.678697$		$h=0.736705$		$h=0.844717$	
	δ	ARL$_1$	SDRL$_1$	ARL$_1$	SDRL$_1$	ARL$_1$	SDRL$_1$	ARL$_1$	SDRL$_1$	ARL$_1$	SDRL$_1$
	0.001	356.362	355.862	258.309	257.809	239.540	239.039	245.595	245.094	253.853	253.353
	0.003	343.633	343.133	198.430	197.929	177.052	176.551	183.767	183.266	193.275	192.774
	0.005	300.370	299.870	103.173	102.672	86.855	86.354	91.775	91.273	99.098	98.596
	0.01	266.414	265.914	69.865	69.363	57.690	57.188	61.310	60.807	66.784	66.282
	0.03	206.710	206.209	38.868	38.365	31.554	31.050	33.700	33.196	36.994	36.491
	0.05	105.162	104.661	14.391	13.882	11.567	11.056	12.387	11.876	13.660	13.150
	0.1	33.146	32.642	4.963	4.435	4.026	3.490	4.296	3.763	4.718	4.189
	0.5	8.048	7.531	2.211	1.636	1.863	1.268	1.962	1.373	2.119	1.540
	1	1.805	1.206	1.298	0.622	1.182	0.464	1.214	0.510	1.267	0.581
PCI		2.124		1.114		1		1.032		1.083	
RMI		3.581		0.177		0		0.052		0.132	

Table 6. *Cont.*

Model	ARFI(2,0.4)										
	UCL	$b_1 = 0.530159$		$b_2 = 0.93074$		$h = 0.690974$		$h = 0.750162$		$h = 0.85915$	
	δ	ARL_1	$SDRL_1$	ARL_1	$SDRL_1$	ARL_1	$SDRL_1$	ARL_1	$SDRL_1$	ARL_1	$SDRL_1$
0.25	0.001	326.213	325.713	256.661	256.161	237.527	237.026	243.556	243.055	252.038	251.538
	0.003	291.333	290.833	196.322	195.821	174.977	174.476	181.583	181.082	191.111	190.610
	0.005	203.842	203.341	101.398	100.897	85.435	84.934	90.210	89.709	97.381	96.880
	0.01	156.563	156.062	68.510	68.008	56.669	56.166	60.168	59.665	65.495	64.993
	0.03	98.753	98.252	38.044	37.541	30.967	30.462	33.034	32.530	36.222	35.719
	0.05	39.115	38.611	14.081	13.572	11.360	10.849	12.147	11.637	13.374	12.864
	0.1	11.812	11.301	4.872	4.343	3.972	3.436	4.231	3.697	4.637	4.106
	0.5	3.694	3.155	2.185	1.610	1.852	1.256	1.947	1.357	2.097	1.517
	1	1.432	0.787	1.293	0.616	1.182	0.464	1.213	0.508	1.263	0.576
	PCI	1.377		1.109		1		1.030		1.080	
	RMI	1.333		0.174		0		0.051		0.129	
λ	Control Chart	EWMA		Modified EWMA		New Modified EWMA					
		$r = 0$		$r = 2$		$r_1 = 2, r_2 = 0.1r_1$		$r_1 = 2, r_2 = 0.4r_1$		$r_1 = 2, r_2 = 0.8r_1$	
	UCL	$b_1 = 0.500171$		$b_2 = 0.924614$		$h = 0.675902$		$h = 0.735894$		$h = 0.849005$	
	δ	ARL_1	$SDRL_1$	ARL_1	$SDRL_1$	ARL_1	$SDRL_1$	ARL_1	$SDRL_1$	ARL_1	$SDRL_1$
0.05	0.0005	368.039	367.539	261.666	261.166	242.670	242.169	248.749	248.248	257.340	256.840
	0.001	365.729	365.229	202.441	201.940	180.508	180.007	187.388	186.887	197.278	196.777
	0.003	356.653	356.153	106.455	105.954	89.358	88.856	94.523	94.022	102.231	101.730
	0.005	347.838	347.338	72.366	71.864	59.518	59.016	63.347	62.845	69.141	68.639
	0.01	326.880	326.380	40.394	39.891	32.623	32.119	34.909	34.405	38.414	37.911
	0.03	256.464	255.964	14.976	14.467	11.957	11.446	12.835	12.324	14.197	13.687
	0.1	117.575	117.074	5.143	4.616	4.138	3.603	4.427	3.895	4.881	4.353
	0.3	20.429	19.923	2.269	1.697	1.893	1.300	2.000	1.414	2.170	1.593
	1	1.557	0.931	1.314	0.643	1.188	0.473	1.223	0.522	1.280	0.598
	PCI	3.421		1.123		1		1.034		1.089	
	RMI	8.485		0.183		0		0.054		0.136	

doi:10.20944/preprints202512.0072.v1

Table 6. *Cont.*

Model	ARFI(2,0.4)										
0.15	UCL	$b_1 = 0.518407$		$b_2 = 0.9398$		$h = 0.688714$		$h = 0.750003$		$h = 0.864163$	
	δ	ARL_1	$SDRL_1$	ARL_1	$SDRL_1$	ARL_1	$SDRL_1$	ARL_1	$SDRL_1$	ARL_1	$SDRL_1$
	0.001	356.810	356.310	259.669	259.169	240.516	240.015	246.677	246.176	255.155	254.655
	0.003	344.229	343.729	199.997	199.496	178.225	177.724	185.050	184.549	194.763	194.262
	0.005	301.387	300.887	104.422	103.921	87.750	87.249	92.769	92.268	100.258	99.757
	0.01	267.658	267.158	70.812	70.311	58.353	57.850	62.051	61.549	67.657	67.155
	0.03	208.156	207.655	39.447	38.944	31.948	31.444	34.145	33.641	37.523	37.020
	0.05	106.347	105.846	14.618	14.109	11.718	11.207	12.558	12.048	13.866	13.356
	0.1	33.659	33.155	5.039	4.511	4.076	3.540	4.352	3.820	4.787	4.258
	0.5	8.200	7.683	2.240	1.666	1.881	1.287	1.983	1.396	2.145	1.567
	1	1.831	1.234	1.308	0.635	1.188	0.473	1.221	0.519	1.275	0.593
PCI		2.144		1.117		1		1.032		1.086	
RMI		3.576		0.180		0		0.053		0.134	
0.25	UCL	$b_1 = 0.531866$		$b_2 = 0.955346$		$h = 0.70173$		$h = 0.764301$		$h = 0.87958$	
	δ	ARL_1	$SDRL_1$	ARL_1	$SDRL_1$	ARL_1	$SDRL_1$	ARL_1	$SDRL_1$	ARL_1	$SDRL_1$
	0.001	326.519	326.019	257.741	257.241	238.829	238.328	244.861	244.360	253.246	252.746
	0.003	292.053	291.553	197.751	197.250	176.338	175.837	183.006	182.505	192.566	192.065
	0.005	205.138	204.637	102.628	102.127	86.381	85.879	91.247	90.745	98.547	98.045
	0.01	157.891	157.390	69.455	68.953	57.355	56.853	60.930	60.428	66.375	65.873
	0.03	99.852	99.351	38.627	38.123	31.369	30.865	33.486	32.983	36.756	36.253
	0.05	39.666	39.162	14.310	13.801	11.512	11.001	12.320	11.810	13.582	13.072
	0.1	12.002	11.491	4.949	4.421	4.022	3.487	4.288	3.755	4.706	4.176
	0.5	3.755	3.216	2.214	1.640	1.870	1.276	1.968	1.380	2.123	1.544
	1	1.446	0.803	1.303	0.629	1.188	0.472	1.220	0.517	1.272	0.588
PCI		1.385		1.113		1		1.031		1.082	
RMI		1.332		0.176		0		0.052		0.131	

5.2. Empirical Application

The U.S. stock prices hold considerable importance in the global financial arena due to the U.S. stock market being the largest, most liquid, and most important market worldwide. Fluctuations in U.S. stock prices not only signify the performance, stability, and profitability of large firms but also act as a predictive indication of macroeconomic circumstances, investor expectations, and worldwide economic mood. The S&P 500, including 500 prominent U.S. corporations, serves as a well-established benchmark that reflects overall market dynamics and is commonly utilized for investment assessment, portfolio management, and policy analysis. Due to their inherent volatility, long-term dependency, and susceptibility to external shocks in stock prices, they present a realistic and demanding context for assessing statistical monitoring techniques. Thus, employing U.S. stock data enables researchers to assess the efficacy of control charts in identifying structural changes, abrupt shifts, or anomalous patterns in actual time series. This study utilizes three U.S. stock price datasets as representative real-world data sources to validate and assess the efficacy of control charts in monitoring process changes. This research makes use of actual data sets, which include the current U.S. stock prices of Walmart (WMT), Amazon.com (AMZN), and Microsoft (MSFT). All three of these companies are members of the S&P 500 indexes. All of these were fitted using the 82^{th} sample of monthly data from January 2019 to October 2025, searched on the $2^{r}d$ of November, 2025. Three different applications of the U.S. stock price datasets were fitted as ARI(p, d) and ARFI(p, d) models using the t-statistics test from the Box-Jenkins technique in the R programming language. The white noise of each model was subsequently checked for its exponential mean using the one-sample Kolmogorov-Smirnov test in SPSS.

Firstly, application 1 was fitted with an ARI$(2, 2)$ model that shows monthly data of the U.S. stock prices of Walmart (WMT) (Unit:USD). These data were obtained from https://th.investing.com/equities/wal-mart-stores-historical-data. The Box-Ljung test indicated that the model was appropriated (Sig $= 0.5512 > 0.05$), and the one-sample Kolmogorov-Smirnov test indicated that the residuals of the ARI$(2, 2)$ model follow an exponential distribution (Sig $= 0.531 > 0.05$). An acceptable way to write the answer is as follows:

$$Y_t = 0.1407 - 0.8145\, Y_{t-1} - 0.4889\, Y_{t-2} + \epsilon_t \quad ; \epsilon_t \sim Exp(2.7137)$$

This is the operator form of the ARI$(2, 2)$ model, with B defined as the backward shift operator.

$$(1 - 0.8145B - 0.4889B^2)(1 - B)^2 Y_t = 0.1407 + \epsilon_t$$

Second, application 2 was fitted with an ARFI$(1, 0.2)$ model that shows monthly data of the U.S. stock prices of Amazon.com (AMZN) (Unit:USD). These data were obtained from https://th.investing.com/equities/amazon-com-inc-historical-data. The Box-Ljung test indicated that the model was appropriated (Sig $= 0.3317 > 0.05$), and the one-sample Kolmogorov-Smirnov test indicated that the residuals of the ARFI$(1, 0.2)$ model follow an exponential distribution (Sig $= 0.177 > 0.05$). The following is a good way to write it:

$$Y_t = 0.9514\, Y_{t-1} + \epsilon_t + ..., \quad ; \epsilon_t \sim Exp(8.2358)$$

Since B is the backward shift operator, this is the operator form of the ARFI$(1, 0.2)$ model.

$$(1 - 0.9514B)(1 - B)^{0.2} Y_t = \epsilon_t$$

Third, application 3 was fitted with an ARFI$(2, 0.4)$ model that shows monthly data of the U.S. stock prices of Microsoft (MSFT) (Unit:USD). These data were obtained from https://th.investing.com/equities/microsoft-corp-historical-data. The Box-Ljung test indicated that the model was appropriated (Sig $= 0.883 > 0.05$), and the one-sample Kolmogorov-Smirnov test indicated that the residuals of the

ARFI$(1, 0.2)$ model follow an exponential distribution (Sig $= 0.925 > 0.05$). An example of an effective style of writing it is:

$$Y_t = 0.9395\, Y_{t-1} + 0.0342\, Y_{t-2}\epsilon_t + ..., \quad ; \epsilon_t \sim Exp(15.0898)$$

In this operator form, B is specified as the backward shift operator, and the ARFI$(2, 0.4)$ model is represented.

$$(1 - 0.9395B - 0.0342B^2)(1 - B)^{0.4} Y_t = \epsilon_t$$

The results of capability of new modified EWMA, modified EWMA, and EWMA charts under ARI$(2, 2)$, ARFI$(1, 0.2)$,and ARFI$(2, 0.4)$ that to showed in Table 7, 8, and 9, respectively. They examined a one-sided control chart with an LCL of 0 and a symmetrically two-sided control chart with an LCL of 0.5, after setting λ equal to 0.05. Take note that the new modified EWMA chart in this section, which is used with the set $r_2 = 0.1r_1$, provides a lower ARL and SDRL than the sets $r_2 = 0.4r_1$ and $r_2 = 0.8r_1$. The findings show that, in every scenario and for every model, the new modified EWMA control chart computed fewer ARL_1 and SDRL_1 values compared to the EWMA control chart and the modified EWMA control chart, both a one-sided and a two-sided chart. Based on the PCI and RMI analysis, the New Modified EWMA control chart demonstrates the highest effectiveness in detecting process shifts for both one-sided and two-sided cases. The Modified EWMA chart performs better than the traditional EWMA chart, which shows the lowest effectiveness among the three. The findings were comparable to those from the simulated data in the preceding section, and they validated the capabilities of the new modified EWMA chart. The graphic representation of the PCI and RMI values for all charts under ARI $(2, 2)$, ARFI $(1, 0.2)$, and ARFI $(2, 0.4)$ clearly demonstrated the capability in Figures 1, 2, and 3.

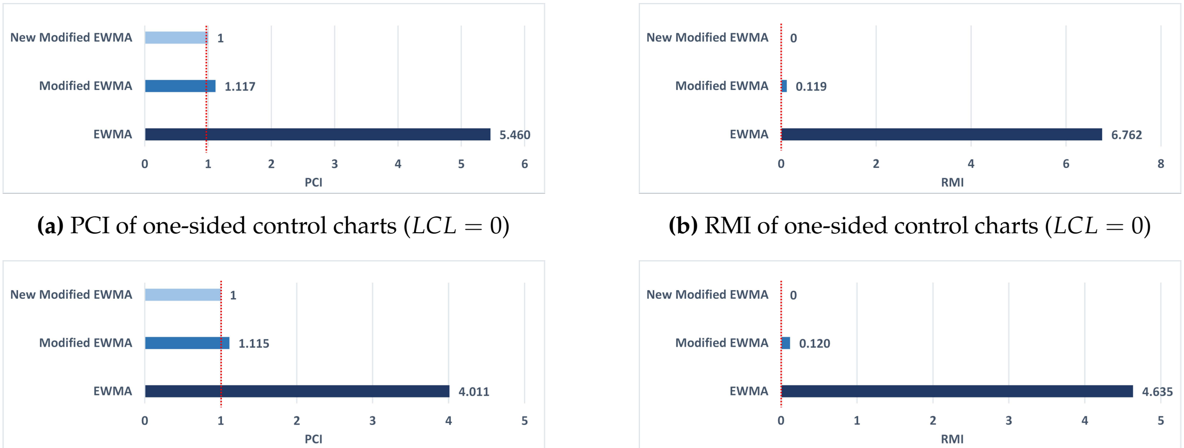

(a) PCI of one-sided control charts ($LCL = 0$) **(b)** RMI of one-sided control charts ($LCL = 0$)

(c) PCI of two-sided control charts ($LCL = 0.5$) **(d)** RMI of two-sided control charts ($LCL = 0.5$)

Figure 1. PCI and RMI of the EWMA, Modified EWMA, and New Modified EWMA control charts under the ARI(2,2) model, based on monthly Walmart (WMT) stock prices. (a)–(b) show one-sided charts ($LCL = 0$), while (c)–(d) present two-sided charts ($LCL = 0.5$).

After that, all control charts were set to $\lambda = 0.05$ in order to identify changes using a two-sided control limit. The EWMA, modified EWMA, and new modified EWMA charts were set to $r_1 = r = 0$, $r_1 = r = 2$, and $r_1 = 2, r_2 = 0.1r_1$, respectively. In addition, the UCL and LCL controls are symmetrically located around the center line of a symmetric control chart, allowing them to detect process changes equally in both directions. Process monitoring is simplified, and balanced performance is assured, even when detecting little changes, due to this symmetry. In order to identify changes in the process mean, three control charts were utilized to fit three datasets of US stock prices using the 82^{th} sample of monthly data from January 2019 to October 2025. These were achieved by fitting the models followed by the above-mentioned assessment.

Table 7. Comparing the capabilities of EWMA, Modified EWMA, and New Modified EWMA control charts, all set with a lower control limit at LCL$= 0$ for one-sided and LCL$= 0.5$ for two-sided control charts, under the ARI$(2,2)$ model using the monthly Walmart stock prices with parameters defined as $\theta = 0.1407$, $\phi_1 = -0.8145$, and $\phi_2 = -0.4889$ and determined $\text{ARL}_0 = 370$.

Model	λ	Control Chart		EWMA		Modified EWMA		New Modified EWMA	
				$r = 0$		$r = 2$		$r_1 = 2, r_2 = 0.1r_1$	
		LCL	UCL	$b_1 = 0.02393$		$b_2 = 5.3503$		$h = 3.84443$	
			δ	ARL_1	SDRL_1	ARL_1	SDRL_1	ARL_1	SDRL_1
ARI(2,2)	0.05	0	0.0005	368.385	367.885	297.371	296.871	287.180	286.680
			0.001	366.764	366.264	248.560	248.059	234.620	234.119
			0.003	360.370	359.870	150.272	149.771	135.688	135.187
			0.005	354.112	353.612	107.876	107.375	95.627	95.126
			0.01	339.040	338.540	63.536	63.034	55.283	54.780
			0.03	286.093	285.593	24.588	24.083	21.085	20.579
			0.1	165.700	165.199	8.504	7.989	7.291	6.773
			0.3	48.054	47.551	3.615	3.075	3.143	2.595
			1	4.872	4.343	1.840	1.243	1.659	1.046
		PCI		5.460		1.117		1	
		RMI		6.762		0.119		0	
		LCL	UCL	$b_1 = 0.60261$		$b_2 = 5.87596$		$h = 4.36282$	
			δ	ARL_1	SDRL_1	ARL_1	SDRL_1	ARL_1	SDRL_1
		0.5	0.001	366.237	365.737	292.438	291.938	281.750	281.250
			0.003	362.045	361.545	241.754	241.253	227.447	226.946
			0.005	346.091	345.591	143.026	142.525	128.692	128.191
			0.01	331.329	330.829	101.757	101.256	89.932	89.431
			0.03	298.849	298.349	59.411	58.909	51.586	51.083
			0.05	210.629	210.128	22.884	22.378	19.610	19.103
			0.1	92.469	91.967	7.975	7.459	6.843	6.323
			0.5	26.007	25.502	3.458	2.915	3.013	2.463
			1	4.526	3.995	1.808	1.209	1.634	1.018
		PCI		4.011		1.115		1	
		RMI		4.635		0.120		0	

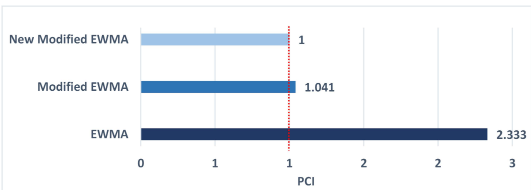

(a) The PCI of one-sided control charts ($LCL = 0$) under the ARFI(1,0.2) model

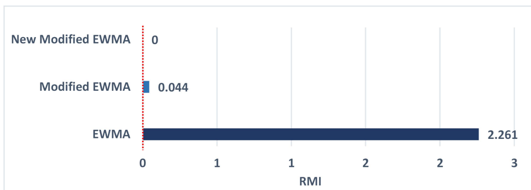

(b) The RMI of one-sided control charts ($LCL = 0$) under the ARFI(1,0.2) model

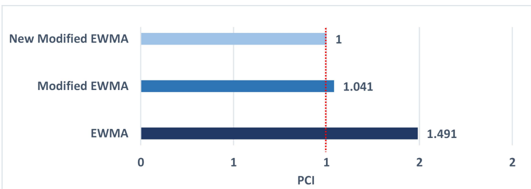

(c) The PCI of two-sided control charts ($LCL = 0.5$) under the ARFI(1,0.2) model

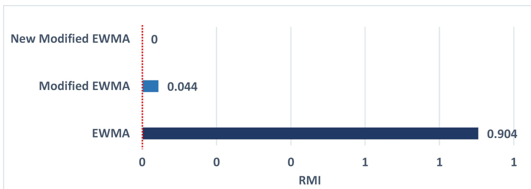

(d) The RMI of two-sided control charts ($LCL = 0.5$) under the ARFI(1,0.2) model

Figure 2. The PCI and RMI values of the EWMA, Modified EWMA, and New Modified EWMA control charts under the ARFI(1,0.2) model are analytical from monthly Amazon.com (AMZN) stock prices. (a) and (b) illustrate the PCI and RMI for the one-sided control charts ($LCL = 0$). (c) and (d) display the PCI and RMI for the two-sided control charts ($LCL = 0.5$).

 doi:10.20944/preprints202512.0072.v1

Table 8. Comparing the capabilities of EWMA, Modified EWMA, and New Modified EWMA control charts, all set with a lower control limit at LCL= 0 for one-sided, and LCL= 0.5 for two-sided control charts, under the ARFI$(1, 0.2)$ model using the monthly Amazon.com stock prices with parameters defined as $\theta = 0$, $\phi_1 = 0.9514$ and determined $\text{ARL}_0 = 370$.

Model	λ	Control Chart		EWMA		Modified EWMA		New Modified EWMA	
				$r = 0$		$r = 2$		$r_1 = 2, r_2 = 0.1r_1$	
ARFI(1,0.2)	0.05	LCL	UCL	$b_1 = 0.36745$		$b_2 = 17.297$		$h = 15.5057$	
		0	δ	ARL_1	SDRL_1	ARL_1	SDRL_1	ARL_1	SDRL_1
			0.0005	359.142	358.642	293.164	292.664	288.881	288.381
			0.001	348.560	348.060	242.517	242.016	236.890	236.389
			0.003	311.673	311.173	143.673	143.172	137.998	137.497
			0.005	281.661	281.161	102.279	101.778	97.564	97.063
			0.01	226.495	225.994	59.760	59.258	56.616	56.113
			0.03	124.740	124.239	23.045	22.540	21.723	21.217
			0.1	44.779	44.276	8.049	7.533	7.595	7.077
			0.3	13.280	12.770	3.501	2.959	3.325	2.781
			1	3.274	2.729	1.834	1.236	1.766	1.163
		PCI		2.333		1.041		1	
		RMI		2.261		0.044		0	
		LCL	UCL	$b_1 = 0.89608$		$b_2 = 17.8242$		$h = 16.0301$	
		0.5	δ	ARL_1	SDRL_1	ARL_1	SDRL_1	ARL_1	SDRL_1
			0.001	338.903	338.403	291.315	290.815	287.333	286.833
			0.003	312.530	312.030	240.121	239.620	234.692	234.191
			0.005	238.302	237.801	141.271	140.770	135.710	135.209
			0.01	192.528	192.027	100.287	99.786	95.667	95.166
			0.03	129.995	129.494	58.439	57.937	55.362	54.860
			0.05	56.362	55.860	22.506	22.000	21.214	20.708
			0.1	18.744	18.237	7.882	7.365	7.437	6.919
			0.5	6.507	5.986	3.451	2.908	3.278	2.733
			1	2.369	1.800	1.823	1.225	1.756	1.153
		PCI		1.491		1.041		1	
		RMI		0.904		0.044		0	

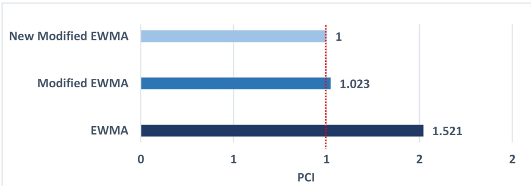

(a) The PCI of one-sided control charts ($LCL = 0$) under the ARFI(2,0.4) model

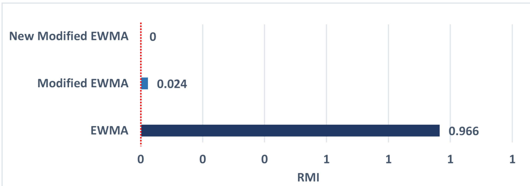

(b) The RMI of one-sided control charts ($LCL = 0$) under the ARFI(2,0.4) model

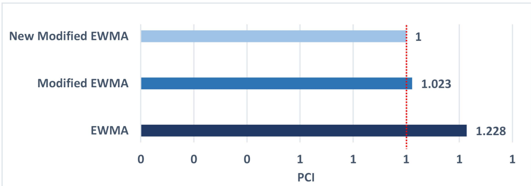

(c) The PCI of two-sided control charts ($LCL = 0.5$) under the ARFI(2,0.4) model

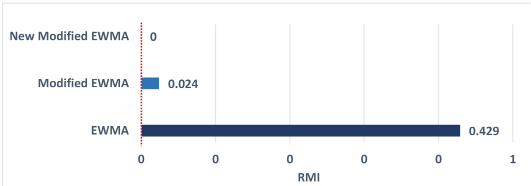

(d) The RMI of two-sided control charts ($LCL = 0.5$) under the ARFI(2,0.4) model

Figure 3. The PCI and RMI values of the EWMA, Modified EWMA, and New Modified EWMA control charts under the ARFI(2,0.4) model are analytical from monthly Microsoft (MSFT) stock prices. (a) and (b) illustrate the PCI and RMI for the one-sided control charts ($LCL = 0$). (c) and (d) display the PCI and RMI for the two-sided control charts ($LCL = 0.5$).

Table 9. Comparing the capabilities of EWMA, Modified EWMA, and New Modified EWMA control charts, all set with a lower control limit at LCL$=0$ for one-sided, and LCL$=0.5$ for two-sided control charts, under the ARFI$(2, 0.4)$ model using the monthly Microsoft stock prices with parameters defined as $\theta = 0$, $\phi_1 = 0.9395$, $\phi_2 = 0.0342$ and determined ARL$_0 = 370$.

Model	λ	Control Chart		EWMA		Modified EWMA		New Modified EWMA	
				$r=0$		$r=2$		$r_1=2, r_2=0.1r_1$	
		LCL	UCL	$b_1=0.71894$		$b_2=31.6416$		$h=29.808$	
ARFI(2,0.4)	0.05	0	δ	ARL$_1$	SDRL$_1$	ARL$_1$	SDRL$_1$	ARL$_1$	SDRL$_1$
			0.0005	341.540	341.040	291.125	290.625	289.381	288.881
			0.001	317.109	316.609	240.017	239.516	237.308	236.807
			0.003	246.505	246.004	141.269	140.768	138.257	137.756
			0.005	201.555	201.054	100.303	99.802	97.757	97.255
			0.01	138.321	137.820	58.458	57.955	56.739	56.237
			0.03	61.027	60.525	22.514	22.009	21.787	21.281
			0.1	20.314	19.808	7.883	7.366	7.632	7.115
			0.3	6.924	6.405	3.450	2.907	3.353	2.809
			1	2.432	1.866	1.822	1.224	1.785	1.183
		PCI		1.521		1.023		1	
		RMI		0.966		0.024		0	
		LCL	UCL	$b_1=1.246041$		$b_2=32.1688$		$h=30.3335$	
		0.5	δ	ARL$_1$	SDRL$_1$	ARL$_1$	SDRL$_1$	ARL$_1$	SDRL$_1$
			0.001	321.083	320.583	290.382	289.882	288.191	287.691
			0.003	283.596	283.096	238.890	238.389	235.878	235.377
			0.005	193.408	192.907	140.029	139.528	136.928	136.427
			0.01	146.825	146.324	99.258	98.757	96.679	96.178
			0.03	91.786	91.284	57.757	57.255	56.038	55.536
			0.05	37.050	36.547	22.227	21.721	21.505	20.999
			0.1	12.447	11.937	7.794	7.276	7.545	7.028
			0.5	4.776	4.247	3.423	2.880	3.327	2.782
			1	2.078	1.497	1.816	1.218	1.779	1.177
		PCI		1.228		1.023		1	
		RMI		0.429		0.024		0	

As is seen in Figure 4, in the case of the ARI$(2, 2)$ model, the new modified EWMA control chart is able to recognize changes for the first time at the 1^{st} samples, whereas the modified EWMA and EWMA charts are able to identify changes for the first time at 21^{st} and 71^{st} samples, respectively. As shown in Figure 5, the new modified EWMA control chart is able to detect changes for the first time at the 1^{st} samples for the ARFI$(1, 0.2)$ model, and the modified EWMA is able to detect changes for the first time at the 8^{th} samples, but the EWMA chart is unable to detect changes inside the 82^{nd} samples. Finally, as shown in Figure 6, the ARFI$(2, 0.4)$ model can be observed with the new modified EWMA control chart at the 1^{st} samples, and with the modified EWMA at the 28^{th} samples as well. However, the EWMA chart fails to detect changes within the 82^{nd} samples of the same ARFI$(1, 0.2)$.

 doi:10.20944/preprints202512.0072.v1

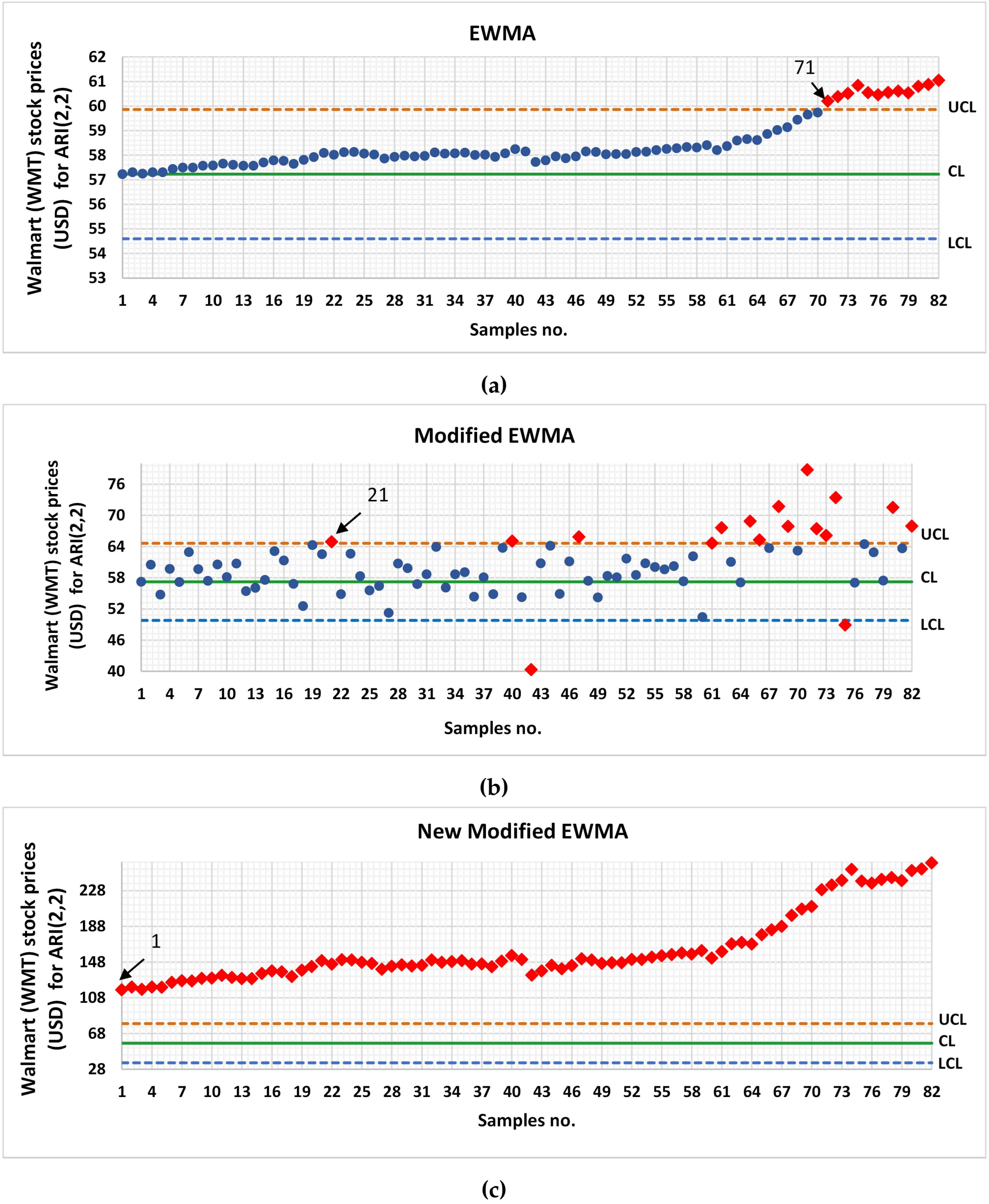

Figure 4. The capability to detect on symmetric two-sided control charts, namely (a) EWMA, (b) Modified EWMA, and (c) New Modified EWMA under the ARI(2,2) model, is demonstrated using the dataset of monthly Walmart (WMT) stock prices.

Preprints.org (www.preprints.org) | NOT PEER-REVIEWED | Posted: 2 December 2025 doi:10.20944/preprints202512.0072.v1

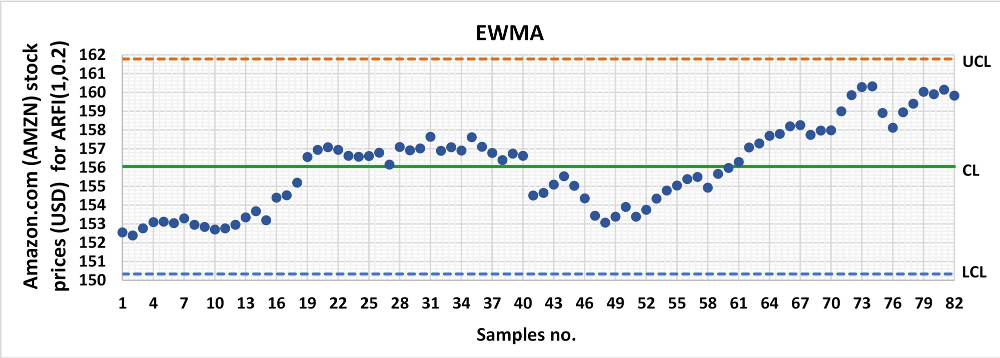

(a)

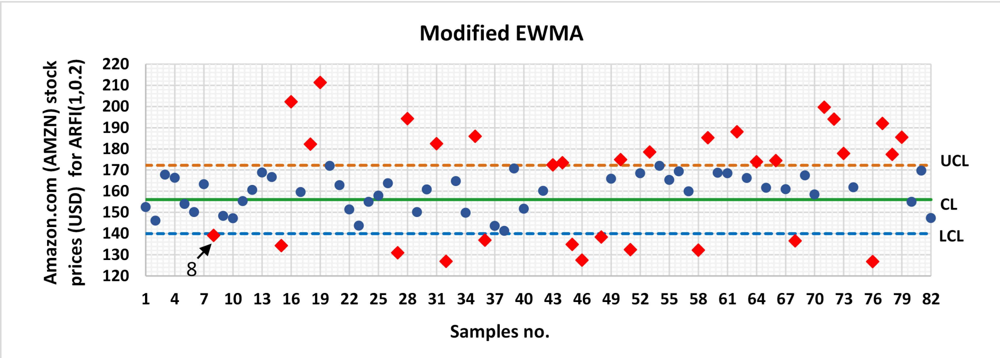

(b)

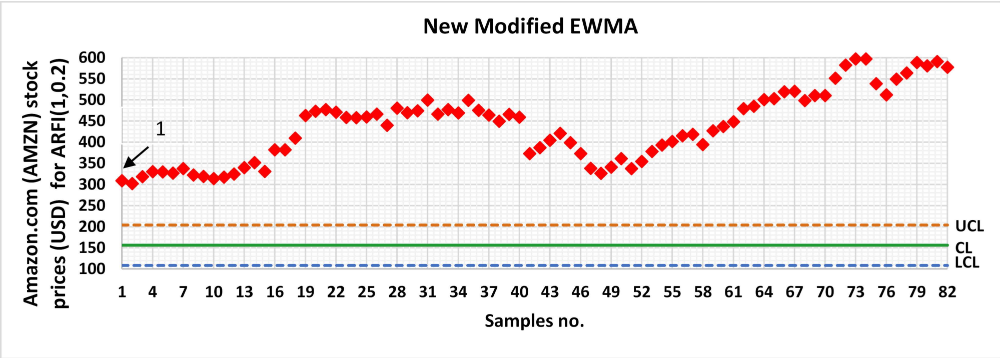

(c)

Figure 5. The capability to detect on symmetric two-sided control charts, namely (a) EWMA, (b) Modified EWMA, and (c) New Modified EWMA under the ARFI(1,0.2) model, is demonstrated using the dataset of monthly Amazon.com (AMZN) stock prices.

 doi:10.20944/preprints202512.0072.v1

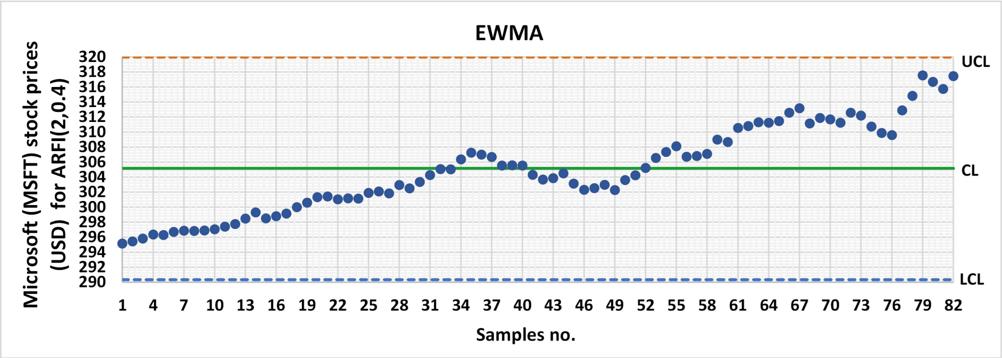

(a)

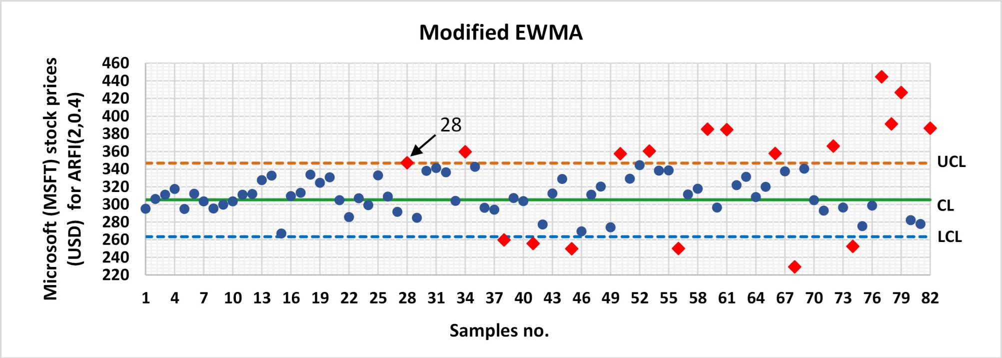

(b)

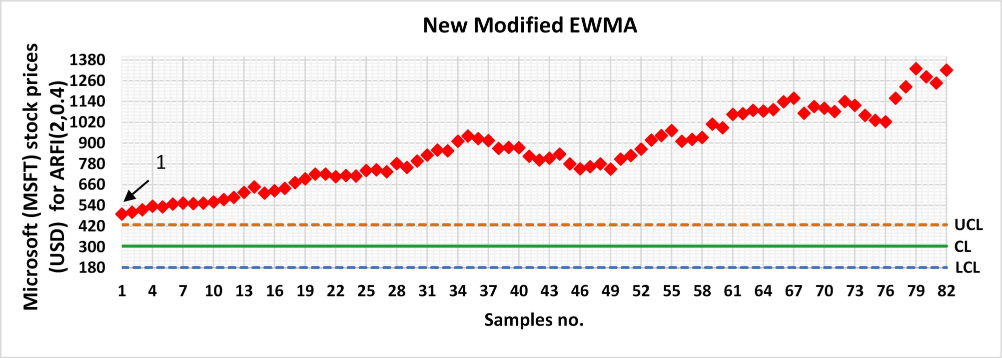

(c)

Figure 6. The capability to detect on symmetric two-sided control charts, namely (a) EWMA, (b) Modified EWMA, and (c) New Modified EWMA under the ARFI(2,0.4) model, is demonstrated using the dataset of monthly Microsoft (MSFT) stock prices.

6. Conclusions

One way to assess a control chart's performance using precise formulae and NIE methods is to examine and analyze the ARL computation. This study used both methods to track the ARI and ARFI models with exponential white noise to compute the ARL on the new modified EWMA chart. In contrast to numerical ARL, which requires much longer computation times, analytical ARL performs better and may be computed instantaneously. In the subsequent step, the ARL was used to compare the EWMA and modified EWMA charts instead of the new modified EWMA chart that was created using an explicit formula. Compared to both the conventional EWMA and the modified EWMA charts, it shows greater capability detection in all tests run under the condition's examination. The findings indicate that the new modified EWMA chart is an effective instrument for detecting minor to moderate shifts utilizing the ARI and ARFI models. Notably, the modified EWMA chart with parameters (r_1, $r_2 = 0.1r_1$) demonstrated the lowest ARL1 and SDRL1 across all scenarios, followed by the modified EWMA chart with ($r_2 = 0.4r_1$), ($r_2 = 0.8r_1$), the modified EWMA, and the standard EWMA charts, respectively. In addition, the ARL_1 values are lower in the new updated EWMA control chart that utilizes r_2 close to r_1, whereas the old control chart uses r_2 much more than r_1. Based on these results, the new modified EWMA control chart—which makes far less use of r_2 than r_1—is a viable alternative to the control charts used to evaluate the effectiveness of the real-world datasets used in this work. Finally, the new modified EWMA control chart's capacity was proved to outperform utilizing actual lift data from the US stock prices dataset under the ARFI and ARI models. Further research will employ several models such as ARIMA, SARIMA, ARFIMA, and SARFIMA to determine the ARL of the revised EWMA control chart using an explicit formula. The reason for this is because data from the actual world and data from simulations are different.

Author Contributions: Conceptualization, K.K. and Y.A.; methodology, K.K.; software, K.K.; validation, Y.A.; formal analysis, K.K.; investigation, K.K.; writing—original draft preparation, K.K.; writing—review and editing, K.K. and Y.A.; visualization, K.K.; supervision, Y.A.; funding acquisition, Y.A.; All authors have read and agreed to the published version of the manuscript.

Funding: This research was funded by the National Science, Research, and Innovation Fund (NSRF) and King Mongkut's University of Technology North Bangkok with Contract no. KMUTNB-FF-69-B-05

Data Availability Statement: This data can be found at https://www.investing.com/equities/united-states.

Acknowledgments: This research was funded by the National Science, Research, and Innovation Fund (NSRF) and King Mongkut's University of Technology North Bangkok with Contract no. KMUTNB-FF-69-B-05

Conflicts of Interest: The authors declare no conflict of interest.

References

1. Malindzakova, M.; Čulková, K.; Trpčevská, J. Shewhart control charts implementation for quality and production management. *Processes* **2023**, *11*, 1246. [CrossRef].
2. Kovarik, M.; Šarga, L.; Klímek, P. Usage of control charts for time series analysis in financial management. *J. Bus. Econ. Manag.* **2015**, *16*, 138–158. [CrossRef].
3. Morrison, L. The use of control charts to interpret environmental monitoring data. *Nat. Areas J.* **2008**, *28*, 66–73. [CrossRef].
4. Suman, G.; Prajapati, D. Control chart applications in healthcare: a literature review. *Int. J. Metrol. Qual. Eng.* **2018**, *9*, 5. [CrossRef].
5. Shewhart, W.A. The application of statistics as an aid in maintaining quality of a manufactured product. *J. Am. Stat. Assoc.* **1925**, *20*, 546–548. [CrossRef].
6. Page, E.S. Continuous inspection schemes. *Biometrika* **1954**, *41*, 100–115. [CrossRef].
7. Roberts, S.W. Control chart tests based on qeometric moving averages. *Technometrics* **1959**, *1*, 239–250. [CrossRef].
8. Patel, A.K.; Divecha, J. Modified exponentially weighted moving average (EWMA) control chart for an analytical process data. *J. Chem. Eng. Mater. Sci.* **2011**, *2*, 12–20. [CrossRef].
9. Khan, N.; Aslam, M.; Jun, C. Design of a control chart using a modified EWMA statistic. *Qual. Reliab. Eng. Int.* **2016**, *33*, 1095–1104. [CrossRef].
10. Silpakob, K.; Areepong, Y.; Sukparungsee, S.; Sunthornwat, R. A new modified EWMA control chart for monitoring processes involving autocorrelated data. *Intell. Autom. Soft Comput.* **2022**, *36*, 281–298. [CrossRef].
11. Sinu, E.; Kleden, M.A.; Atti, A. Application of ARIMA model for forecasting national economic growth: A focus on gross domestic product data. *Barekeng J. Ilmu Mat. Terap.* **2024**, *18*, 1261–1272. [CrossRef].
12. Hrithik, P.M.; Rehman, M.Z.; Dar, A.A.; Wangmo, A.T. Forecasting CO_2 emissions in India: A time series analysis using ARIMA. *Processes* **2024**, *12*, 2699. [CrossRef].
13. Pan, J.N.; Chen, S.T. Monitoring long-memory air quality data using ARFIMA model. *Environmetrics* **2008**, *19*, 209–219. [CrossRef].
14. Rabyk, L.; Schmid, W. EWMA control charts for detecting changes in the mean of a long-memory process. *Metrika* **2016**, *79*, 267–301. [CrossRef].
15. Hyung, N.; Franses, P.H. Forecasting time series with long memory and level shifts. *J. Forecast.* **2005**, *24*, 1–16. [CrossRef].

16. Champ, C.W.; Rigdon, S.E. A comparison of the Markov chain and the integral equation approaches for evaluating the run length distribution of quality control charts. *Commun. Stat. Simul. Comput.* **1991**, *20*, 191–204. [CrossRef].
17. Fu, M.C.; Hu, J. Efficient design and sensitivity analysis of control charts using Monte Carlo simulation. *Management Science* **1999**, *45*, 395–413. [CrossRef].
18. Phanyaem, S. Explicit Formulas and Numerical Integral Equation of ARL for SARX(P,r)$_L$ Model Based on CUSUM Chart. *Mathematics and Statistics* **2022**, *10*, 88–99. [CrossRef].
19. Suriyakat, W.; Petcharat, K. Exact run length computation on EWMA control chart for stationary moving average process with exogenous variables. *Math. Stat.* **2022**, *10*, 624–635. [CrossRef].
20. Chananet, C.; Phanyaem, S. Improving CUSUM control chart for monitoring a change in processes based on seasonal ARX model. *IAENG Int. J. Appl. Math.* **2022**, *52*, IJAM_52_3_08. [CrossRef].
21. Bualuang, D.; Peerajit, W. Performance of the CUSUM control chart using approximation to ARL for long-memory fractionally integrated autoregressive process with exogenous variable. *Appl. Sci. Eng. Prog.* **2023**, *16*, 5917. [CrossRef].
22. Peerajit, W. Developing average run length for monitoring changes in the mean in the presence of long memory under seasonal fractionally integrated MAX model. *Math. Stat.* **2023**, *11*, 34–50. [CrossRef].
23. Riaz, M.; Abbas, Z.; Nazir, H.Z.; Abid, M. On the development of triple homogeneously weighted moving average control chart. *CSymmetry* **2021**, *13*, 360. [CrossRef].
24. Sunthornwat, R.; Sukparungsee, S.; Areepong, Y. Analytical explicit formulas of average run length of homogeneously weighted moving average control chart based on a MAX process. *Symmetry* **2023**, *15*, 2112. [CrossRef].
25. Karoon, K.; Areepong, Y.; Sukparungsee, S. Modification of ARL for detecting changes on the double EWMA chart in time series data with the autoregressive model. *Connection Science* **2023**, *35*, 2219040. [CrossRef].
26. Karoon, K.; Areepong, Y. Enhancing the performance of an adjusted MEWMA control chart running on trend and quadratic trend autoregressive models. *Lobachevskii Journal of Mathematics* **2024**, *45*, 1601–1617. [CrossRef].
27. Karoon, K.; Areepong, Y. The efficiency of the new extended EWMA control chart for detecting changes under an autoregressive model and its application. *Symmetry* **2025**, *17*, 104. [CrossRef].
28. Peerajit, W.; Areepong, Y. Alternative to detecting changes in the mean of an autoregressive fractionally integrated process with exponential white noise running on the modified EWMA control chart. *Processes* **2023**, *11*, 503. [CrossRef].
29. Neammai, J.; Sukparungsee, S.; Areepong, Y. Analytical assessment of the DMEWMA control chart for detecting shifts in ARI and ARFI models with applications. *Symmetry* **2025**, *17*, 1889. [CrossRef].
30. Mcleod, I.; Hipel, K.W. Simulation procedures for Box–Jenkins models. *Water Resour. Res.* **1978**, *14*, 969–975. [CrossRef].
31. Almousa, M. Adomian decomposition method with modified Bernstein polynomials for solving nonlinear Fredholm and Volterra integral equations. *Math. Stat.* **2020**, *8*, 278–285. [CrossRef].
32. Fonseca, A.; Ferreira, P.H.; Nascimento, D.C.; Fiaccone, R.; Correa, C.U.; Piña, A.G.; Louzada, F. Water particles monitoring in the Atacama desert: SPC approach based on proportional data. *Axioms* **2021**, *10*, 154. [CrossRef].
33. Alevizakos, V.; Chatterjee, K.; Koukouvinos, C. The triple exponentially weighted moving average control chart for monitoring Poisson process. *Quality and Reliability Engineering International* **2023**, *38*, 532–549. [CrossRef].